



Assisting and eliminating memory effects of paste by adding polysaccharidesRyu Baba * and Kazuhiro Fujimaki [†]*Department of Aerospace Engineering, College of Science and Technology, Nihon University, Funabashi 274-8501, Japan*Chihiro Uemura *Department of Space and Astronautical Science, School of Physical Science,
SOKENDAI (The Graduate University for Advanced Studies), Sagamihara 252-5210, Japan,
and DigitalBlast, Inc., Tokyo 101-0051, Japan*Yousuke Matsuo  and Akio Nakahara [‡]*Laboratory of Physics, College of Science and Technology, Nihon University, Funabashi 274-8501, Japan*Akinori Muramatsu *Department of Aerospace Engineering, College of Science and Technology, Nihon University, Funabashi 274-8501, Chiba, Japan*

(Received 26 June 2023; accepted 12 October 2023; published 3 November 2023)

A densely packed colloidal suspension, called a paste, is known to remember the direction of its motion because of its plasticity. Because the memory in the paste determines the preferential direction for crack propagation, the desiccation crack pattern morphology depends on memory of its motions (memory effect of paste). Two types of memory effects are memory of vibration and memory of flow. When a paste is dried, it usually shows an “isotropic and random cellular” desiccation crack pattern. However, when a paste is vibrated before drying and it remembers the direction of its vibrational motion, primary desiccation cracks propagate in a direction perpendicular to its vibrational motion before drying (memory of vibration). Once it flows and remembers the direction of its flow motion, primary desiccation cracks propagate in the direction parallel to its flow motion (memory of flow). Anisotropic network formation via interparticle attraction among colloidal particles in a suspension is the dominant factor affecting a paste’s memory of its motion. Calcium carbonate (CaCO_3) paste remembers the direction of its vibrational motion, but not its own flow direction because Coulombic repulsion among charged CaCO_3 colloidal particles prevents the formation of a network structure in a flow. For this study, we strove to assist and eliminate CaCO_3 paste memory effects by adding polysaccharides. First, to characterize memory in paste, we propose a method of image analysis to quantify the strength and the direction of the anisotropy of desiccation crack patterns using Shannon’s information entropy. Next, we conduct experiments to add polysaccharide to CaCO_3 paste, revealing that the addition of a small amount of polysaccharide to CaCO_3 paste assists the paste in remembering its own flow motion. Findings also indicate that the addition of a large amount of polysaccharide prevents the formation of both memories of its flow and vibrational motion and eliminates the memory effects of paste. We then perform “floculation and sedimentation” experiments to investigate the interaction among CaCO_3 colloidal particles in a solution. Results show that, in an aqueous solution with low polysaccharide concentration, CaCO_3 colloidal particles flocculate each other and quickly form a sediment in a short time, whereas, in an aqueous solution with high polysaccharide concentration, a longer time is necessary for flocculation and sedimentation. Because the addition of small amounts of polysaccharides to CaCO_3 paste induces polymer bridging between colloidal particles as interparticle attraction, it helps to produce a macroscopic network structure which retains memory of its flow motion and thereby assists the formation of memory of flow, whereas the addition of large amounts of polysaccharides induces interparticle repulsion, which prevents the formation of memory effects of all types.

DOI: [10.1103/PhysRevE.108.054602](https://doi.org/10.1103/PhysRevE.108.054602)**I. INTRODUCTION**

Crack formations are often random and stochastic phenomena, and thereby they are difficult to control. For example,

*Present address: Sanwa Comsys Engineering Corporation, Tokyo 166-0003, Japan.

[†]Present address: Acty System, Hamamatsu 433-8108, Japan.

[‡]Corresponding author: nakahara.akio@nihon-u.ac.jp

fracture phenomena under strong impacts are accompanied by the rapid development of cracks. In such cases, predicting when and where the first crack appears is difficult. Moreover, predicting how cracks propagate and break a material into fragments is also difficult. To avoid unexpected and dangerous situations, attempts to control crack formation are important topics in various fields of science and technology.

Some regularities of fracture phenomena have been reported. If a glass is dropped on the floor, then cracks will

develop rapidly and the glass will shatter into pieces. At first glance, the glass fragments will appear to have been broken into pieces randomly, but in fact the size distribution of the fragments obeys a scaling law [1–3]. Regularity in crack formation is not limited to these statistical scaling laws. The crack morphology can be controlled in the case of quasistatic fracture formation. By varying the cooling rate of a quenched thin glass plate, various crack patterns can be created in a controlled manner, including straight, meandering (oscillatory), and branching patterns [4–7].

Columnar joints of cooled lava are other examples of controlled crack patterns that are formed in nature. A regular array of prismatic columns is formed along a cooling direction of lava. A similar columnar joint structure is obtainable by drying a thick paste, i.e., a mixture of starch powder and water [8–13]. Because a thick paste in a container dries from the top surface, cracks first occur at the top surface. These cracks propagate vertically downwards toward the bottom of the thick paste. Thereby, columnar joints of dried starch paste are formed vertically. However, with no preferential direction of cooling or drying, only “isotropic and random cellular” crack patterns are considered to be formed in nature and laboratories [13–15].

For studies supporting our research, we have investigated how anisotropic crack patterns are formed according to the memory effect of paste when a thin paste is dried homogeneously in space. For a thin paste, cracks can be regarded to propagate along a horizontal direction and the morphology of plumose structure observed on the side view of desiccation cracks indicates in which direction the desiccation crack propagated horizontally. The final spacing among desiccation cracks in dried thin paste is about equal to the paste thickness [13–17].

Here a paste is a densely packed colloidal suspension with plasticity, and the value of its yield stress quantifies the strength of its plasticity. A dilute colloidal suspension can be regarded as a Newtonian viscous fluid without plasticity, and the value of its yield stress remains zero. As the value of the solid volume fraction in paste increases, the value of its viscosity increases, and, above the liquid limit, the value of its yield stress becomes positive, and its yield stress is now an increasing function of the solid volume fraction [18]. Thus, the liquid limit corresponds to the onset of pastry behavior. We also note that the value of the yield stress diverges when the solid volume fraction approached to the plastic limit, and above the plastic limit we cannot mix too much colloidal particles with less water homogeneously in space, and the mixture is in a semisolid state like a half-dried cookie which contains many gas bubbles inside. Therefore, the colloidal suspension can be regarded as a viscoplastic fluid, called a paste, when the value of its solid volume fraction is between the liquid limit and plastic limit [19–24].

When an external force is applied to a paste before it dries, the paste remembers the external force it received even after one stops applying the external force, which causes controlled desiccation cracks to appear as the water in the paste evaporates. This phenomenon is designated as the “memory effect of paste.” The plasticity of paste enables it to remember its motion in the form of plastic deformation. There are two types of memory effect: memory of vibration and memory

of flow. When a paste remembers the direction of its vibrational motion, primary desiccation cracks propagate in the direction perpendicular to its vibrational motion before drying (memory of vibration). By contrast, when a paste remembers the direction of its flow motion, primary desiccation cracks propagate in the direction parallel to its flow motion (memory of flow). Interparticle interaction among colloidal particles plays important roles in forming the memories of each type [13,25–40]. It has also been demonstrated that crack formation can be controlled not only by the memory effect of paste but also by application of electric and magnetic fields to the paste at the moment of drying [41–48].

As described herein, we investigate the effects of adding polysaccharides to calcium carbonate (CaCO_3) paste on the memory effect of a paste. The motivation for undertaking this research is investigation of the effect of adding a dilatant fluid to a paste which shows a memory effect. A highly concentrated starch paste is known to be a typical dilatant fluid, which shows shear-thickening behavior, i.e., the fluid viscosity increases rapidly as the applied stress is increased [19–24,49,50]. First, we mix starch colloidal particles with CaCO_3 paste and find that, by adding starch colloidal particles to CaCO_3 paste that remembers its vibrational motion but which has no memory of its flow motion, the paste gets the ability to remember its flow motion. As our study continues, it becomes readily apparent that, even when we did not add colloidal particles of starch to CaCO_3 paste but added only water-soluble starch to CaCO_3 paste, the paste also gains the ability to remember its flow motion. Moreover, the findings indicate that, by adding a large amount of water-soluble starch to CaCO_3 paste, the paste loses its ability to remember any motion: it can remember neither vibration nor flow. As a result, the shear-thickening effect is not necessary for assisting and eliminating memory effects of paste. Added soluble polysaccharides influence the interparticle interaction among colloidal particles in paste, and thus they assist or eliminate memory effects of paste, depending on the amounts of polysaccharides added to the paste.

This paper is organized as follows. First, in Sec. II we review the memory effect of paste and explain the difference between memory of vibration and memory of flow. In Sec. III for the quantitative evaluation of the anisotropy of desiccation crack patterns induced by memory effects of paste, we propose a method of image analysis to characterize the strength and the direction of the anisotropy of these crack patterns using Shannon’s information entropy. Using image analysis, one can also evaluate the time evolution of the anisotropy of crack patterns induced by memory effects. As described in Sec. IV, systematic experiments are conducted to elucidate the effects of adding starch colloidal particles to CaCO_3 paste. In Sec. V other systematic experiments are conducted to elucidate the effects of adding water-soluble saccharide to CaCO_3 paste. Moreover, we change the molecular weights of saccharides added to CaCO_3 paste using saccharides of different types such as water-soluble starch, dextrin, and glucose. Then we study the effects of saccharide polymer length on the memory effect. As described in Sec. VI, “floculation and sedimentation” experiments are conducted to study the interparticle interaction among CaCO_3 colloidal particles in each saccharide solution. Section VII presents discussion of

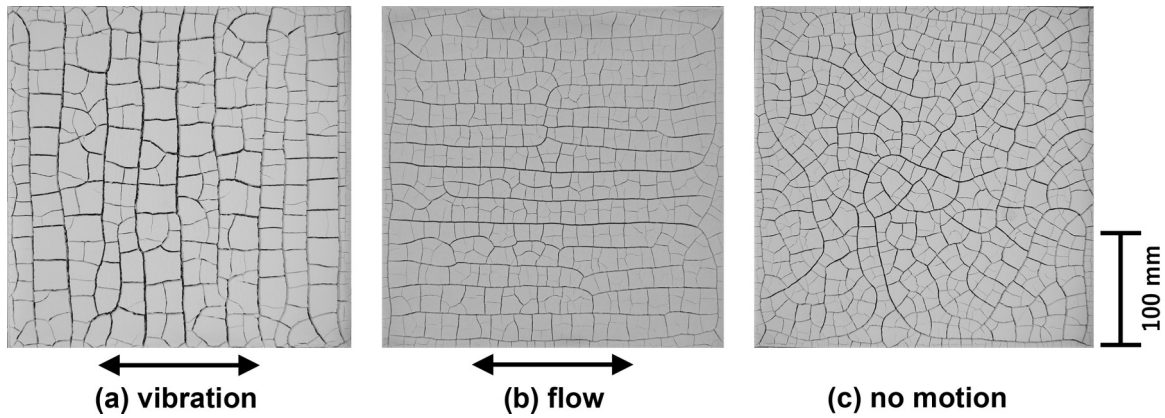


FIG. 1. Desiccation crack patterns of a paste produced by mixing colloidal particles of magnesium carbonate hydroxide with water. Each square acrylic container is 300 mm on each side. In (a) and (b), a container in which a paste is stored is vibrated before drying along the double-headed arrow with the amplitude of $r = 15$ mm and the frequency of $f = 110$ rpm for 1 min. Consequently, the maximum strength of the absolute value of the acceleration induced by horizontal vibration is 2.0 m/s^2 . In (c), the container is not vibrated before drying. Because we use 225 g of colloidal particles to make a paste for (a) and 150 g to make a paste for (b) and (c), the final thickness of each paste after drying is proportional to the mass of colloidal particles per unit area and are 6.0 mm in (a) and 4.0 mm in (b) and (c). (a) Striped desiccation crack pattern with memory of vibration, obtained by vibrating a water-poor high-plastic paste horizontally before drying. The solid volume fraction of the paste at the time of vibration is $\rho = 12.5\%$. Primary desiccation cracks propagate in the direction perpendicular to the vibration that the paste experienced before drying. (b) Striped desiccation crack pattern with a memory of flow, obtained by vibrating a water-medium low-plastic paste which flows under vibration. The solid volume fraction of the paste at the time of vibration is $\rho = 7.7\%$. Primary desiccation cracks propagate along a flow motion induced by vibration of the container. (c) “Isotropic and random cellular” desiccation crack pattern with no memory of its motions, obtained merely by drying a water-rich viscous paste with the solid volume fraction $\rho = 2.0\%$. Because its solid volume fraction is less than the value of liquid limit of 4.0%, the water-rich viscous paste has no plasticity; it cannot remember any of its motions, even if vibrated before drying.

the mechanism by which a small amount of added polysaccharides assists CaCO_3 paste to remember its flow motion, although a large amount of added polysaccharides eliminates CaCO_3 paste memory of any of its motions. Finally, our results are summarized in Sec. VIII.

II. MEMORY EFFECT OF PASTE

This section presents a review of the memory effects of paste and presents an explanation of the difference between two memories (memory of vibration and memory of flow), and how interactions among colloidal particles play their roles in the respective memory effects.

A. Anisotropic desiccation crack patterns produced by paste memory effects

When a paste comprising colloidal particles and water is dried, “isotropic and random cellular” desiccation crack patterns appear. Such cracks are often observed at dried-up ponds. However, if a paste is vibrated horizontally before drying, then a striped desiccation crack pattern appears; the crack pattern morphology depends on the direction of its vibrational motion. This pattern reflects the “memory effect of paste” [25,26].

In fact, memory effects are of two types: memory of vibration and memory of flow [27]. Figure 1 portrays typical desiccation crack patterns that form when we dry pastes of magnesium carbonate hydroxide. These pastes are produced by mixing colloidal particles of magnesium carbonate hydroxide (Kanto Chemical Co. Inc., Tokyo, Japan) with distilled water. Colloidal particles of magnesium carbonate hydroxide

are solid and difficult to dissolve in water. The density of the magnesium carbonate hydroxide is 2.0 g/cm^3 , the shape of each colloidal particle of magnesium carbonate hydroxide is disklike, and the median diameter of colloidal particles of magnesium carbonate hydroxide is $3.0 \mu\text{m}$, as is shown in Fig. 2(a). Yield stress of magnesium carbonate hydroxide paste is measured by using a dynamic stress rheometer (Rheometrics, Piscataway, NJ), and the result is presented in Fig. 2(b). Since these colloidal particles are not charged in water and attract each other via interparticle attractive force, magnesium carbonate hydroxide paste has a strong plasticity with small values of the liquid limit and plastic limit [25–27,31].

The inner size of each square acrylic container presented in Fig. 1 is $300 \text{ mm} \times 300 \text{ mm}$. The masses of colloidal particles and volume of water in each paste are, respectively, 225 g and 788 ml in Fig. 1(a), 150 g and 900 ml in Fig. 1(b), and 150 g and 1500 ml in Fig. 1(c). Therefore, the initial values of the solid volume fraction of the paste before drying are $\rho = 12.5\%$ in Fig. 1(a), $\rho = 7.7\%$ in Fig. 1(b), and $\rho = 2.0\%$ in Fig. 1(c), respectively. The pastes portrayed in Figs. 1(a) and 1(b) are vibrated horizontally with the amplitude of $r = 15$ mm and frequency of $f = 110$ rpm for 1 min before drying. Therefore, the maximum strength of the absolute value of the acceleration induced by horizontal vibration is 2.0 m/s^2 in Figs. 1(a) and 1(b), whereas the paste in Fig. 1(c) is not vibrated before drying.

In Fig. 1 are striped desiccation crack patterns of two types: one is induced by memory of vibration and the other by flow, and an “isotropic and random cellular” desiccation crack pattern with no memory of its motion. First, Fig. 1(a)

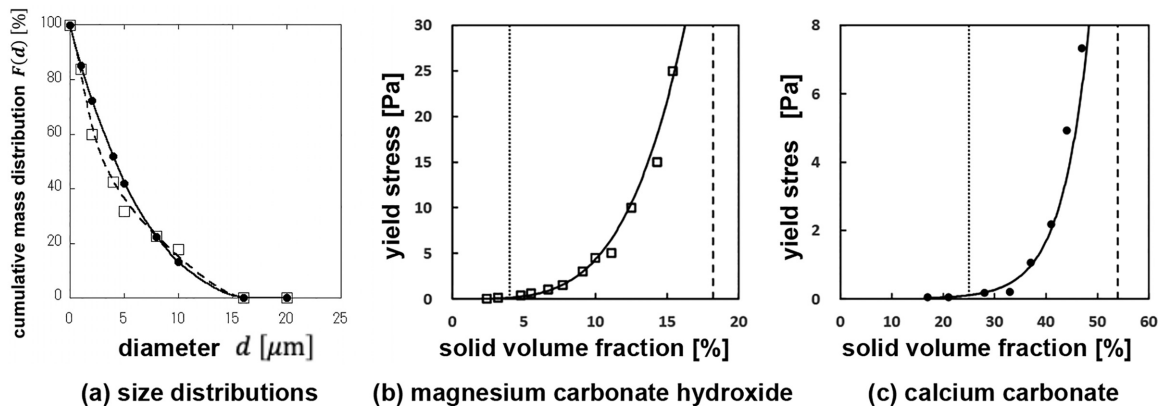


FIG. 2. Size distributions of colloidal particles in pastes and yield stresses of pastes. (a) Cumulative mass distribution of colloidal particles, i.e., a mass fraction of colloidal particles with its diameter larger than the value of d . Data of magnesium carbonate hydroxide are denoted by open squares and a broken line and its median diameter is given by $3.0\ \mu\text{m}$, while data of calcium carbonate are denoted by solid circles and a solid line and its median diameter is given by $4.0\ \mu\text{m}$. (b), (c) Yield stresses of magnesium carbonate hydroxide paste in (b) and CaCO_3 paste in (c), shown as a function of its solid volume fraction. The dotted lines denote liquid limit and broken lines denote plastic limit of each paste. The colloidal suspension can be regarded as a viscoplastic fluid, called a paste, when the value of its solid volume fraction is between the liquid limit and plastic limit. Note that the values of liquid limit and plastic limit of CaCO_3 paste are larger than those of magnesium carbonate hydroxide paste because the plasticity of CaCO_3 paste is weakened by Coulombic repulsion between charged colloidal particles [25–27,31].

shows that, when a water-poor paste is vibrated, it remembers the direction of its vibrational motion. Desiccation cracks propagate in the direction perpendicular to the direction of its vibrational motion. This phenomenon is known as “memory effect of vibration.” By contrast, when a water-medium paste is vibrated, it flows rather than vibrates. Once it flows, it remembers the direction of its flow motion. Desiccation cracks propagate along a direction parallel to its flow direction, as presented in Fig. 1(b). This phenomenon is called “memory effect of flow.” These pastes have plasticity to retain memories of their motions, i.e., such as vibration or flow. However, as for a water-rich paste with its solid volume fraction less than the value of liquid limit, the paste has no plasticity and is unable to remember any of its motion. Therefore, when a paste with no memory is dried, desiccation cracks take only “isotropic and random cellular” structures, as presented in Fig. 1(c).

B. Morphological phase diagrams of desiccation crack patterns which reflect memory effects

Magnesium carbonate hydroxide and calcium carbonate (CaCO_3) are typical powders which show different types of memory effects of paste. For example, a paste of magnesium carbonate hydroxide shows both memories of vibration and flow, whereas CaCO_3 paste shows only memory of vibration and it cannot remember its flow direction. To understand the difference in memory effects between two pastes, we would like to present a comparison between the two.

First, let us see the memory effect of a paste of magnesium carbonate hydroxide, which is made by mixing colloidal particles of magnesium carbonate hydroxide with distilled water. Figure 3(a) shows a morphological phase diagram of desiccation crack patterns of pastes of magnesium carbonate hydroxide, which have been vibrated horizontally immediately before drying. The paste behaves as a viscoplastic fluid when its solid volume fraction is between the liquid limit and plastic limit. Also, Fig. 3(a) shows that the desiccation crack

patterns of these viscoplastic pastes of magnesium carbonate hydroxide can be divided into four types, respectively corresponding to regions A, B, C, and D in the morphological phase diagram.

The black solid curve in Fig. 3 represents a yield stress line, on which the value of the maximum shear stress induced by the external horizontal vibration equals that of the yield stress of the paste. In region A below the yield stress line, a water-poor viscoplastic paste with a high solid volume fraction is stored in a container, the container is vibrated horizontally, but the value of the shear stress induced by the external horizontal vibration is smaller than that of the yield stress of the paste. Then the paste is not deformed even under the external horizontal vibration of the container, and thereby only “isotropic and random cellular” desiccation cracks appear after drying.

By contrast, in region B above the yield stress line, a water-poor viscoplastic paste with a high solid volume fraction is stored in a container, the container is vibrated horizontally, and the value of the shear stress induced by the external horizontal vibration exceeds that of the yield stress of the paste. Then the paste is deformed plastically under the external horizontal vibration of the container. It remembers the direction of its vibrational motion, and all primary desiccation cracks propagate in a direction perpendicular to its vibrational motion, illustrating the memory effect of vibration.

In region C a water-medium viscoplastic paste with a medium solid volume fraction is stored in a container, and the container is vibrated horizontally. Then the paste flows rather than vibrates because of the low viscoplasticity of the paste. Once it flows, it remembers its flow direction and all primary desiccation cracks propagate along a flow direction induced by the external horizontal vibration of the container, thereby illustrating the memory effect of flow.

In region D a water-medium viscoplastic paste with a medium solid volume fraction is stored in a container, but

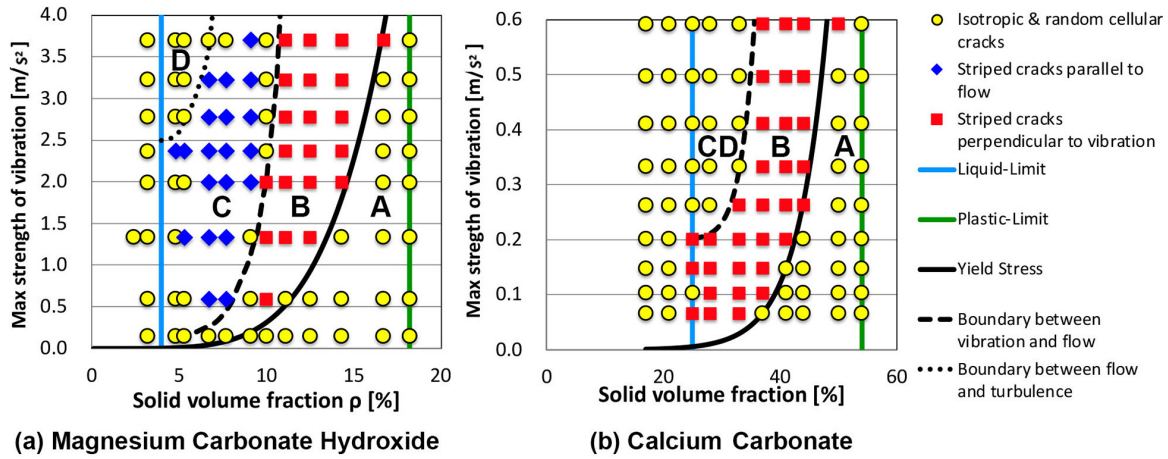


FIG. 3. Morphological phase diagrams of desiccation crack patterns of pastes, expressed as functions of a solid volume fraction ρ of solid colloidal particles in each paste, and the strength of a horizontal vibration, expressed as a maximum acceleration $4\pi^2 r f^2$. Here r represents the amplitude; f represents a frequency of the vibration that pastes have experienced for 1 min before drying. Each acrylic square container is 200 mm on each side. The final thickness of each paste after drying is about 7 mm. Open circles filled with yellow denote “isotropic and random cellular” desiccation crack patterns. Also, blue solid diamonds denote striped desiccation crack patterns, the direction of which is parallel to the direction of a flow induced by the vibration. Red solid squares denote striped desiccation crack patterns, the direction of which is perpendicular to the direction of its vibrational motion. A light-blue solid vertical line shows the liquid limit of the paste. The green solid vertical line shows the plastic limit of the paste. The black solid curve represents a yield stress line, on which the value of the maximum shear stress induced by the horizontal vibration equals that of the yield stress of the paste. A black broken curve represents a boundary between the vibrational motion and flow motion of paste. The black dotted curve represents a boundary between striped cracks parallel to the flow and “isotropic and random cellular” cracks induced by turbulent flow motion. (a) Magnesium carbonate hydroxide. Because the anisotropy of desiccation crack patterns depends on the direction of its vibrational motion in region B and that of its flow motion in region C, the paste of magnesium carbonate hydroxide remembers the directions of its vibrational motion and its flow motion. (b) Calcium carbonate. Because the anisotropy of desiccation crack patterns depends on the direction of its vibrational motion in region B, the $CaCO_3$ paste remembers the direction of its vibrational motion. However, because we obtain “isotropic and random cellular” desiccation crack patterns when the paste flows in region CD, the $CaCO_3$ paste cannot remember the direction of its flow motion [25–27].

the container is vibrated too strongly in a horizontal direction. Then the turbulent flow appears inside the paste; the desiccation cracks become a random-like desiccation crack pattern, the direction of which might reflect the turbulent flow direction.

In a region located left of liquid limit line, a water-rich viscous paste with a low solid volume fraction below the liquid limit is stored in a container, and the container is vibrated horizontally. Because of the lack of the plasticity, the paste cannot remember any of its motions; only “isotropic and random cellular” desiccation crack patterns appear [27].

The memory effect of $CaCO_3$ paste is produced by mixing colloidal particles of calcium carbonate (Kanto Chemical Co. Inc., Tokyo, Japan) with distilled water. Colloidal particles of calcium carbonate are solid and difficult to dissolve in water. The calcium carbonate density is 2.72 g/cm^3 . The shape of each colloidal particle of calcium carbonate is like a rough sand particle. The median diameter of colloidal particles of calcium carbonate is $4.0 \mu\text{m}$, as is shown in Fig. 2(a). Yield stress of $CaCO_3$ paste is presented in Fig. 2(c). Since these colloidal particles are charged positively in water and repel each other via Coulombic repulsive force, $CaCO_3$ paste has a weaker plasticity with larger values of liquid limit and plastic limit. Figure 3(b) portrays a morphological phase diagram of desiccation crack patterns of $CaCO_3$ pastes, which have been vibrated horizontally immediately before drying.

In region A below the yield stress line, a water-poor viscoplastic $CaCO_3$ paste with a high solid volume fraction is stored in a container, the container is vibrated horizontally, but the value of the shear stress induced by the external horizontal vibration is smaller than that of the yield stress of the paste. Then the $CaCO_3$ paste is not deformed even under the external horizontal vibration of the container, so desiccation cracks take “isotropic and random cellular” structures with no memory of motion. By contrast, in region B above the yield stress line, the value of the shear stress induced by the external horizontal vibration exceeds that of the yield stress of the $CaCO_3$ paste. Then the paste is deformed plastically under the external horizontal vibration of the container. Therefore, $CaCO_3$ paste also remembers the direction of its vibrational motion, and all primary desiccation cracks propagate in a direction perpendicular to its vibrational motion, illustrating the memory effect of vibration.

However, results in Fig. 3(b) show that $CaCO_3$ paste cannot remember its flow direction. When a water-medium paste with a medium solid volume fraction is vibrated, it flows rather than vibrates, but, even though it flows, only “isotropic and random cellular” desiccation crack patterns appear, as shown in region CD where uniform flow or turbulent flow appear, depending on the strength of the external vibration. Therefore, we consider that $CaCO_3$ paste cannot remember its flow motion [25,26].

C. Interparticle interactions necessary for memory effects

The major difference between the magnesium carbonate hydroxide paste and CaCO_3 paste is that colloidal particles of magnesium carbonate hydroxide are not charged in water and that magnesium carbonate hydroxide paste can remember its flow motion as in region C of Fig. 3(a), whereas CaCO_3 colloidal particles are charged in water and CaCO_3 paste cannot remember its flow motion, as presented in Fig. 3(b).

Regarding the memory of vibration, almost all pastes remember vibrational motion because, in a water-poor paste with a high solid volume fraction, colloidal particles are densely packed and are located nearby. Thereby, even for charged colloidal particles, the short-ranged van der Waals interparticle attraction becomes the most dominant interaction rather than long-ranged Coulombic repulsion among charged colloidal particles. A macroscopic network structure is formed by interparticle attraction among colloidal particles, and it is considered that memories of vibration and flow are kept in different forms of anisotropic network structures of colloidal particles.

Recently, it was shown that a water-poor paste remembers the direction of its vibrational motion as a form of an anisotropic dense network structure of colloidal particles [39]. X-ray computerized tomography observation and image analysis were performed to the 3D arrangements of colloidal particles in Lycopodium paste which remembers the direction of its vibrational motion. Here the diameters of Lycopodium colloidal particles are approximately $30\ \mu\text{m}$, so we can capture the shapes and positions of colloidal particles clearly. First, an anisotropic structure is induced mainly in the lower part of a layer of the paste [39], because the lower layer of the paste suffers a shear deformation when the container is vibrated horizontally [13,37]. Second, by quantifying the anisotropy in arrangements of neighboring colloidal particles, it was shown that there are more neighboring colloidal particles in the direction perpendicular to the vibration of the container. Since spatial arrangement of colloidal particles becomes a striped pattern which extends in the perpendicular direction of the vibration, anisotropic interstices also extend in the direction perpendicular to the vibration, and thus they play a role as a path of air penetration causing anisotropic crack growth in the direction perpendicular to the vibration [39].

Regarding the memory of flow, the necessary condition for a paste to remember its flow motion is that colloidal particles are not charged in water. For a situation in which a paste can flow, the value of the solid volume fraction of paste is medium and not so high, colloidal particles are not so densely packed, and the mean distance among colloidal particles is not so small. Consequently, the long-ranged Coulombic repulsion becomes the most dominant interaction if colloidal particles are charged in water. In such a situation, it becomes difficult for CaCO_3 paste to maintain a dilute network structure, especially when CaCO_3 paste is deformed strongly under flow motion. For this reason, CaCO_3 paste cannot remember its flow motion. By contrast, colloidal particles of magnesium carbonate hydroxide are not charged in water. The short-ranged van der Waals interparticle attraction among colloidal particles is still a dominant interparticle interaction.

Therefore, they can maintain a dilute network structure even when elongated along a flow direction. For this reason, paste of magnesium carbonate hydroxide can remember its flow motion [32]. We conjecture that spatial arrangement of colloidal particles becomes a striped pattern which extends in the direction parallel to its flow because the dilute network structure is elongated along the flow direction. CT observation is under preparation to reveal the spatial arrangement of colloidal particles in a paste with a memory of flow.

To assist CaCO_3 paste in remembering its flow motion, we merely need to add a small amount of sodium chloride (NaCl) to the CaCO_3 paste. Then the long-ranged Coulombic repulsion of CaCO_3 colloidal particles is screened. Also, the short-ranged van der Waals interparticle attraction among CaCO_3 colloidal particles becomes the dominant interparticle interaction even when the solid volume fraction of the paste is medium and the paste can flow. Thereby, dilute network structures are not broken and can be elongated along the flow direction. They retain the information related to their flow motions. As a result, the interparticle attraction must be a dominant interaction for a paste to remember its flow motion [32].

III. IMAGE ANALYSIS TO CHARACTERIZE CRACK PATTERN ANISOTROPY

In this section we present a method of image analysis for which we use Shannon's information entropy to characterize the anisotropy of desiccation crack patterns induced by memory effects of paste. Then we apply our image analysis to anisotropic desiccation crack patterns induced by memory effects and quantitatively evaluate the anisotropy of desiccation crack patterns and the strength of memories stored in these pastes.

A. Method to characterize crack pattern anisotropy using Shannon's information entropy

Ideas for the evaluation of the anisotropy of crack patterns have been realized in two ways: the estimation of the orientation of fragments and that of cracks which surround each fragment. First, the orientation of fragments is derived by assuming each fragment to be an ellipse and by estimating the orientation of major axis of these ellipses as an angle distribution [51]. In another method, the anisotropy of the orientation of each crack is analyzed by regarding each crack fragment as a nematic liquid molecule and by calculating an order parameter that is related to the mean orientation of the director of nematic liquid molecules [52].

To characterize the anisotropy of striped desiccation crack patterns made of "long and straight" primary cracks induced by memory effects of paste, we herein propose a method by which we adopt Shannon's information entropy to characterize the anisotropy of crack patterns [53,54]. When a paste remembers the direction of its vibrational motion, primary desiccation cracks propagate in the direction perpendicular to the direction of its vibrational motion before the drying process, whereas primary desiccation cracks propagate in the direction parallel to the flow motion when a paste remembers the direction of its flow motion. After these primary cracks are

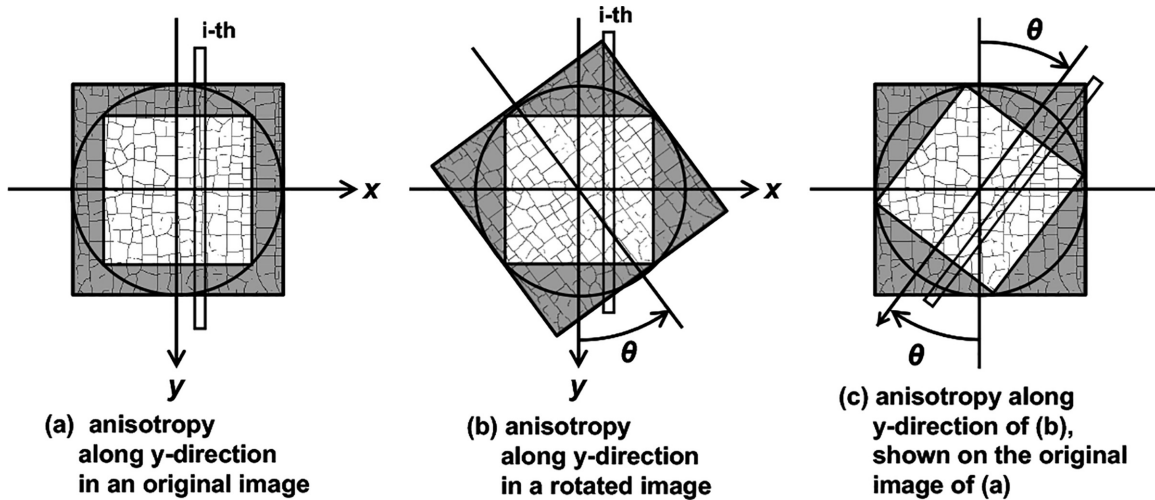


FIG. 4. Method of calculating Shannon’s information entropy S , which characterizes the anisotropy of a striped desiccation crack pattern from its original gray-scale image data. Shannon’s information entropy S is defined to detect the existence of “long and straight” primary cracks which propagate along the y direction. (a) The initial arrangement of an original gray-scale image in xy space. In the original gray-scale image, cracks are denoted as black or dark gray pixels. The original gray-scale image data are binarized and thinned, then black and white inversion of the image data is performed. Finally, cracks are drawn by white pixels; noncrack domains are drawn by black pixels [Figs. 5(b)–5(d) present the final processed images]. Shannon’s information entropy S is defined by $S = -\sum_{i=1}^m \frac{n_i}{N} \log_2 \frac{n_i}{N}$, where n_i denotes the number of white pixels in the i th column at a distance x_i from the y axis; N denotes the total number of white pixels in the whole image, expressed as $N = \sum_{i=1}^m n_i$. Usually we set the width of each i th column as 1 pixel, but we can set their widths as more than 1 for coarse graining. (b) Derivation of the anisotropy in the y direction in a rotated image. The crack pattern anisotropy is systematically calculated by rotating the image by the integral multiple of $\Delta\theta = 1^\circ$ counterclockwise around the center of the image to investigate the angle θ dependence of the anisotropy of the striped crack pattern made of “long and straight” primary cracks. If one merely rotates the square image, then the directions of four sides of the square image deviate from x and y directions, thereby it becomes difficult to calculate Shannon’s information entropy. Therefore, instead of analyzing the whole image, only the small square region inscribed inside the inscribed circle of the whole square image is analyzed to derive Shannon’s information entropy S . After rotating the whole square image by the integral multiple of $\Delta\theta = 1^\circ$ counterclockwise around the center of the image, directions of the four sides of this small square region are reset along the x direction or y direction; its circumscribed circle equals the inscribed circle of the rotated whole square image. Using this method, the value of Shannon’s information entropy S decreases in the direction of the “long and straight” primary cracks. Therefore, the angle dependence of Shannon’s information entropy and the direction of the striped crack pattern can be derived. (c) Schematic image of the process (b) shown on the original image (a). For process (b), the original image is rotated counterclockwise by angle θ ; the anisotropy of the crack pattern is estimated along the y direction of (b). In (c) we represent this process (b) on the original image (a), then the anisotropy of crack pattern is estimated along a direction which is rotated by angle θ clockwise from the vertical y direction of (a).

formed, secondary cracks emerge in a later stage of the drying process, but the directions of these secondary cracks are not determined by memory effects. Instead, secondary cracks are formed to cut long rectangles of striped structure into smaller fragments. It is noteworthy that the primary cracks are much longer than the secondary cracks which emerge in the later stage. Also the primary cracks are far fewer than the secondary cracks [26]. When a paste does not remember any of its motions and the paste is dried homogeneously in space, many desiccation cracks can propagate in any direction; only an “isotropic and random cellular” crack pattern is formed. Therefore, if we simply average the orientation of cracks by number, then the existence of a few primary cracks is ignored when compared with many secondary cracks or many cracks in an “isotropic and random cellular” crack pattern with no memory effects. Therefore, we propose a third method by which we use Shannon’s information entropy to detect the formation of “long and straight” primary cracks induced by memory effects of paste.

Figure 4 portrays a schematic diagram of how Shannon’s information entropy is calculated from photographs of

desiccation crack patterns. In the original gray-scale image, cracks are denoted as black or dark gray pixels, as shown in Figs. 1(a)–1(c). To evaluate the anisotropy of striped crack patterns produced by the memory effect, first we transform the original gray-scale image to a binarized image, subsequently performing line thinning processing using the Zhang-Suen thinning algorithm to crack lines [55]; then black and white inversion is applied to the image data. Finally, cracks are drawn by white lines composed of white pixels; noncrack domains are drawn with black pixels, as shown in Figs. 5(b)–5(d). Figures 1(a)–1(c) are original gray-scale images with “dark-gray cracks and light-gray noncrack domains”; Figs. 4(a)–4(c) and Fig. 5(a) are schematic representations of how we deal with “binarized and thinned images” with “black crack lines and white noncrack domains.” Also, Figs. 5(b)–5(d) are final processed images with “white crack lines and black noncrack domains” that we obtain after we perform “black and white inversion” to “binarized and thinned images.” If necessary, we perform median blur to remove background noise because of nonuniform lightening before transforming the original gray-scale image to a binarized image.

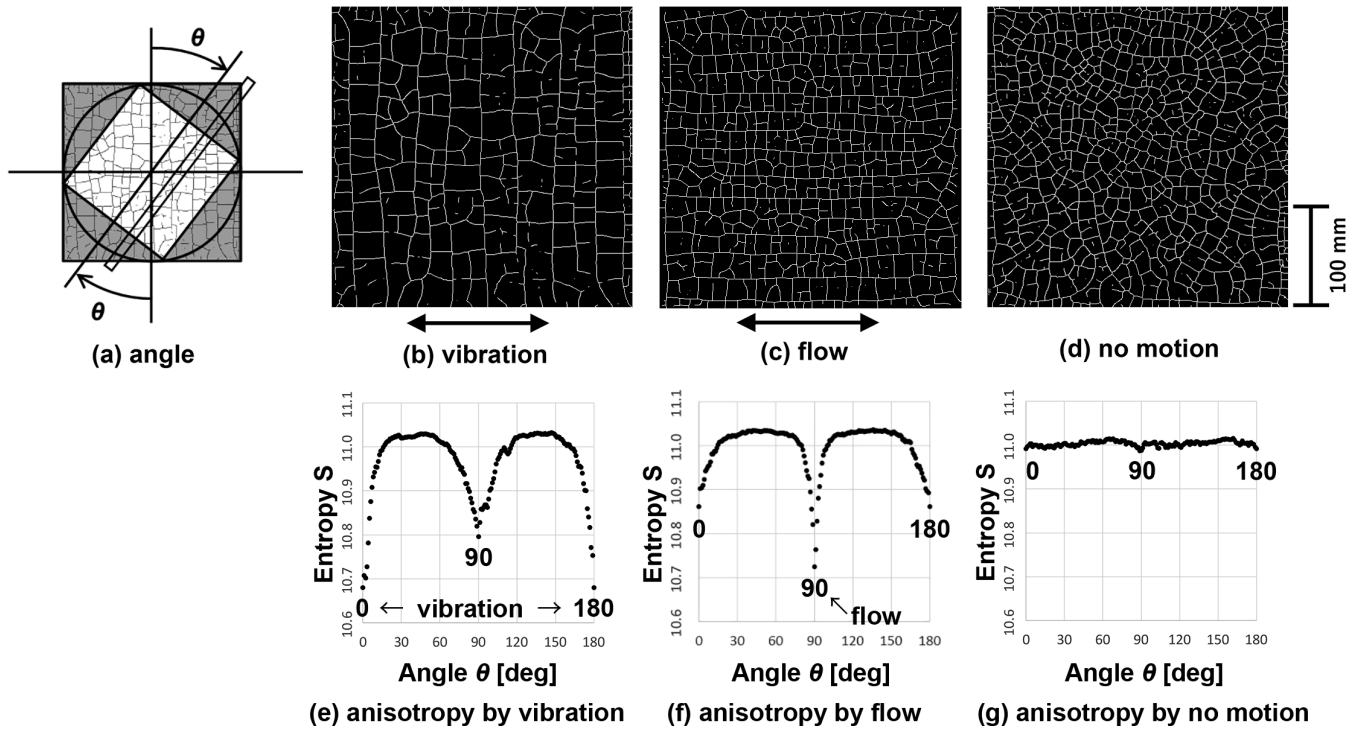


FIG. 5. Calculation of Shannon’s information entropy S , which characterizes the crack pattern anisotropy from its original gray-scale image data presented in Figs. 1(a)–1(c). (a) Angle θ of the direction along which we calculate Shannon’s information entropy S and estimate the preference for cracks to propagate. Therefore, Shannon’s information entropy S is expressed as a function of angle θ to characterize the direction of anisotropic striped crack pattern. Panels (b)–(d) show processed images for the calculation of Shannon’s information entropy S . On the original gray-scale image presented in Fig. 1, cracks are drawn as black or dark gray pixels. As we apply image processing, the original gray-scale data are binarized and thinned. Then “black and white inversion” is applied to the image data. Finally cracks are drawn by white pixels; noncrack domains are drawn with black pixels. If necessary, we perform median blur to remove background noise caused by nonuniform lightening before we transform the original gray-scale image to a binarized image. (b) Processed image of a striped crack pattern with “long and straight” primary cracks along the longitudinal direction, which was presented as Fig. 1(a) and which is induced by the memory of vibration in the “right and left” directions. (c) Processed image of a striped crack pattern with “long and straight” primary cracks along the “right and left” directions, which was presented as Fig. 1(b) and which is induced by the memory of flow in the “right and left” direction. (d) Processed image of an “isotropic and random cellular” crack pattern with no memory of its motion, which was presented as Fig. 1(c). Panels (e)–(g) show Shannon’s information entropies S as functions of an angle θ calculated from processed images of panels (b)–(d). (e) Shannon’s information entropy S calculated from image (b) of longitudinal striped cracks induced by memory of vibration. The global minima of S at $\theta = 0^\circ$ and $\theta = 180^\circ$ correspond to “long and straight” primary cracks in the longitudinal direction ($\theta = 0^\circ$ and 180°) induced by the memory of vibration in the “right and left” direction ($\theta = 90^\circ$). The local minimum of S at $\theta = 90^\circ$ corresponds to many short secondary cracks in the “right and left” directions, which are perpendicular to longitudinal “long and straight” primary cracks. (f) Shannon’s information entropy S calculated from image (c) of striped cracks along the “right and left” direction induced by memory of flow. The global minimum of S at $\theta = 90^\circ$ corresponds to “long and straight” primary cracks in the “right and left” direction ($\theta = 90^\circ$) induced by the memory of flow ($\theta = 90^\circ$). The local minima of S at $\theta = 0^\circ$ and 180° correspond to many short secondary cracks in the longitudinal direction, which are perpendicular to “long and straight” primary cracks in the “right and left” directions. (g) Shannon’s information entropy S calculated from image (d) of “isotropic and random cellular” cracks. For an “isotropic and random cellular” crack pattern, there is no global minimum of S , which means that there is no “long and straight” primary crack: the paste has no memory of its motions.

The size of square photographic image is m pixels \times m pixels. The x axis and y axis, respectively, correspond to the rightward direction and the downward direction in the square image, as denoted in Fig. 4(a). Also, I_{ji} represents the binarized intensity of the final processed image at a position (x_i, y_j) , where $i = 1, 2, \dots, m$ and $j = 1, 2, \dots, m$. Consequently, if $I_{ji} = 1$ (white), then the pixel at a position (x_i, y_j) corresponds to a point on a white crack line. Also, if $I_{ji} = 0$ (black), then the pixel at a position (x_i, y_j) corresponds to a point inside a black noncrack domain.

For example, Fig. 4(a) represents an original gray-scale image of a striped desiccation crack pattern produced by memory

of vibration. Here the paste was vibrated in the x direction before drying. All primary desiccation cracks propagate in the y direction, which is perpendicular to the direction of its vibrational motion. Of course, these “long and straight” cracks in the y direction do not appear without memory effect of paste. Therefore, we would like to use the following method to find the rare event of the formation of “long and straight” primary cracks which propagate in the y direction in Fig. 4(a).

To extract the anisotropy of striped crack patterns made of “long and straight” primary cracks which propagate along the y direction, first we define P_i as the probability that a white pixel, which represents a point on a white crack line, is located

on the i th column at a distance x_i from the reference y axis. As depicted in Fig. 4(a), the number of white pixels in the i th longitudinal column is expressed as

$$n_i = \sum_{j=1}^m I_{ji}. \quad (3.1)$$

Also, the total number of white pixels in the whole image is expressed,

$$N = \sum_{i=1}^m n_i = \sum_{i=1}^m \sum_{j=1}^m I_{ji}. \quad (3.2)$$

Therefore, probability P_i is obtained as

$$P_i = \frac{n_i}{N}. \quad (3.3)$$

When a value of P_k at a certain k is large, and when values of P_i at different columns (i.e., with $i \neq k$) almost vanish, many white pixels are concentrated in the k th longitudinal column: a “long and straight” crack propagates in the y direction along the k th longitudinal column at x_k , and almost no cracks are formed in the different columns. Because a “long and straight” crack propagates in a longitudinal y direction along a certain longitudinal column, we realize that formation of a striped crack pattern is a kind of a deterministic process by which cracks are forced to propagate in a particular direction because of memory effects of the paste. However, when values of P_i at any i th column are almost equal, we realize that crack formation is a random stochastic process by which cracks can propagate in any direction.

To distinguish these two processes, i.e., a deterministic process of anisotropic striped crack formation induced by memory effects of paste and a stochastic process of “isotropic and random cellular” crack formation, we use Shannon’s information entropy S to characterize these processes because the information I_i of an event i with probability of P_i is expressed in terms of binary digits as

$$I_i = -\log_2 P_i. \quad (3.4)$$

Shannon’s information entropy S is introduced as the average level of information I_i by the following equation [53,54]:

$$S = \sum_{i=1}^m P_i I_i = - \sum_{i=1}^m P_i \log_2 P_i = - \sum_{i=1}^m \frac{n_i}{N} \log_2 \frac{n_i}{N}. \quad (3.5)$$

Using the method presented above, we can calculate Shannon’s information entropy S of binarized images of anisotropic crack patterns using Eq. (3.5). When the value of Shannon’s information entropy S of a crack pattern is smaller than those of “isotropic and random cellular” crack patterns, it means that the crack pattern is anisotropic and there are “long and straight” primary cracks which propagate along the y direction because of the memory of vibration.

However, when the paste was vibrated not in the x direction but in a different direction, “long and straight” primary cracks propagate along a direction perpendicular to the direction of the vibration, but not along the y direction, which is perpendicular to the x direction. In this case there are no “long and straight” cracks along the y direction. Therefore, when the

paste was vibrated not in the x direction but in a different direction, the calculation of Shannon’s information entropy cannot characterize the anisotropy of striped crack patterns induced by the memory effect of vibration. To overcome the difficulty explained above, the crack pattern anisotropy is calculated systematically by rotating the image by $\Delta\theta = 1^\circ$ counterclockwise around the center of the image to investigate the angle θ dependence of the direction of “long and straight” primary cracks. Of course, if we just rotate the square image, then the directions of four sides of the square image become different from the x and y directions, as depicted in Fig. 4(b). To avoid such a difficulty, instead of analyzing the whole image, we restrict the region of the image to which we apply our method of image analysis and come to analyze only the small square region inside the whole image. Here the directions of four sides of this small square region are always set as along the x and the y direction. Its circumscribed circle is equal to the inscribed circle of the rotated original whole image. If we represent this process on the original image in Fig. 4(a), then the anisotropy of crack pattern is estimated along a direction which is rotated by angle θ clockwise from the vertical y direction of Fig. 4(a), as depicted in Fig. 4(c). By this calculation, the value of Shannon’s information entropy S decreases at angle θ of the direction of the “long and straight” primary cracks. Therefore, we can derive the angle θ dependence of the direction of striped crack patterns and estimate the type of memory, i.e., vibration or flow, and the strength of the memory effects.

B. Results of image analysis of anisotropic striped crack patterns induced by memory effects of paste

As described in this subsection, we perform image analysis by which we use Shannon’s information entropy to characterize the anisotropy of desiccation crack patterns induced by paste memory effects. As examples, we apply our image analysis to the desiccation crack patterns presented in Fig. 1. The results are shown in Fig. 5.

First, Fig. 5(a) shows an angle θ of the direction along which we calculate Shannon’s information entropy S , which is expressed as a function of angle θ , to characterize the direction of the anisotropic striped crack pattern. Then we can estimate the preferential direction for cracks to propagate. Figures 5(b)–5(d) show processed images for the calculation of Shannon’s information entropy S . On the original gray-scale image presented in Fig. 1, cracks are drawn as black or dark gray pixels. Because the inner size of each acrylic container in Fig. 1 is 300 mm \times 300 mm, as a first step in our image analysis, we rescale the size of the image data to be proportional to its real size and then rescale the inner size of the container in which a paste is stored as 3000 pixels \times 3000 pixels. Then the original gray-scale data are binarized and thinned, “black and white inversion” is applied to the image data. Finally, cracks are drawn using white pixels; noncrack domains are drawn using black pixels.

Figure 5(b) shows a processed image of the striped crack pattern with “long and straight” primary cracks along the longitudinal direction, which was presented as Fig. 1(a) and which is induced by the memory of vibration in “right and left” direction. Next, Fig. 5(c) portrays a processed image

of the striped crack pattern with “long and straight” primary cracks along the “right and left” direction, which was presented as Fig. 1(b) and which is induced by the memory of flow in the “right and left” direction. Figure 5(d) depicts a processed image of an “isotropic and random cellular” crack pattern with no memories of its motion, which was presented as Fig. 1(c). Finally, Figs. 5(e)–5(g) show Shannon’s information entropies S as functions of an angle θ calculated from processed images of Figs. 5(b)–5(d).

In the original gray-scale image [Fig. 1(a)] and its processed image [Fig. 5(b)], where a water-poor paste was vibrated in the “right and left” directions before drying and where the resultant crack pattern obeys the memory effect of vibration, “long and straight” primary cracks propagate in longitudinal direction, the direction of which is perpendicular to the vibration in “right and left” direction. We also find that many short secondary cracks propagate in the direction perpendicular to these “long and straight” primary cracks to cut long rectangles into smaller pieces: few primary “long and straight” cracks propagate in the longitudinal direction perpendicular to its vibrational motion, although many short secondary cracks propagate in the “right and left” direction. Because “long and straight” primary cracks propagate along a longitudinal direction, if we calculate Shannon’s information entropy S of the processed image Fig. 5(b), then we obtain a very small value of S .

If we rotate the image Fig. 5(b) counterclockwise as depicted in Fig. 4(b), then the direction of “long and straight” primary cracks deviates from the longitudinal y direction and the value of S increases. This process of image analysis can also be described in a different way: “If we rotate the direction along which we calculate the value of S clockwise in Fig. 5(b), as shown in Figs. 4(c) and 5(a), then the direction along which we calculate the value of S deviates from the direction of longitudinal “long and straight” primary cracks and the value of S increases.” However, as we continue to increase the angle θ of rotation, the value of S starts to decrease again and takes a small value again at $\theta = 90^\circ$, as portrayed in Fig. 5(e). This is true because the existence of many short secondary cracks can also decrease the value of S . We realize that the value of S at $\theta = 90^\circ$ is just a local minimum. The value of S at the local minimum $\theta = 90^\circ$ is larger than that of the global minimum of S at $\theta = 0^\circ$. It is also noteworthy that the value of S at $\theta = 180^\circ$ becomes equal to that of $\theta = 0^\circ$ because of the definition of S by Eq. (3.5). Therefore, Shannon’s information entropy S defined by Eq. (3.5) can detect the existence of “long and straight” primary cracks along the longitudinal direction and then quantifies “the strength and the direction of the anisotropy of striped crack pattern” and “the strength of memory of vibration” by calculating the value of the global minimum of S . Calculation of S can also detect many short secondary cracks along the “right and left” direction and distinguish secondary cracks from primary cracks by comparing a local minimum with a global minimum in a graph of S as a function of the angle θ .

In the original gray-scale image Fig. 1(b) and its processed image Fig. 5(c), where a container is vibrated in the “right and left” direction before drying, a water-medium paste flows in the same “right and left” direction. The resultant crack pattern obeys the memory effect of flow, i.e., “long and straight”

primary cracks propagate in the “right and left” direction, the direction of which is parallel to the flow in the “right and left” direction. We also found that many short secondary cracks propagate in the longitudinal direction perpendicular to these “long and straight” primary cracks to cut long rectangles into smaller pieces: few primary “long and straight” cracks propagate in the “right and left” direction parallel to its flow motion, while many short secondary cracks propagate in the longitudinal direction. Because many short secondary cracks propagate along the longitudinal direction, if we calculate Shannon’s information entropy S of the image Fig. 5(c), then we get a not too small but the small value of S induced by many short secondary cracks.

If we rotate the image Fig. 5(c) counterclockwise as depicted in Fig. 4(b), then the direction of many short secondary cracks deviates from the longitudinal y direction; the value of S increases. However, as we continue to increase the angle θ of rotation, the direction of “long and straight” primary cracks approaches the longitudinal direction, the value of S starts to decrease strongly and takes a global minimum value at $\theta = 90^\circ$, as portrayed in Fig. 5(f). Here we realize that the value of S at $\theta = 0^\circ$ is just a local minimum. The value of S at the local minimum $\theta = 0^\circ$ is larger than that of the global minimum of S at $\theta = 90^\circ$. Therefore, Shannon’s information entropy S defined by Eq. (3.5) can detect the existence of “long and straight” primary cracks along the “right and left” direction and can quantify the strength of the anisotropy of the striped crack pattern and the strength of memory of flow by calculating the value of the global minimum of S . Calculation of S can distinguish secondary cracks from primary cracks by comparing a local minimum with a global minimum in a graph of S as a function of the angle θ .

Figure 5(d) corresponds to a processed image of an “isotropic and random cellular” desiccation crack pattern of dried paste with no memories of its motion. A paste is water-rich without plasticity. It can remember no motion it experienced. When we examine the value of Shannon’s information entropy S of these “isotropic and random cellular” cracks as a function of the angle θ of rotation in Fig. 5(g), it is apparent that the value of Shannon’s information entropy S merely fluctuates. It has no global minimum or local minimum that corresponds to an anisotropic crack pattern with “long and straight” primary cracks and numerous short secondary cracks.

Therefore, by calculating the values of Shannon’s information entropy S of crack patterns as functions of the angle θ of rotation, we can characterize the desiccation crack pattern anisotropy and can quantify the strengths of memories in pastes.

C. Time evolution of striped crack pattern formation induced by paste memory effects

As described in this subsection, we apply image analysis to the time evolution of the formation of anisotropic desiccation crack patterns induced by memory effects of paste. As an example, Fig. 6 presents results of our image analysis that we performed for striped desiccation crack patterns induced by the memory of flow, as presented already in Figs. 1(b) and 5(c).

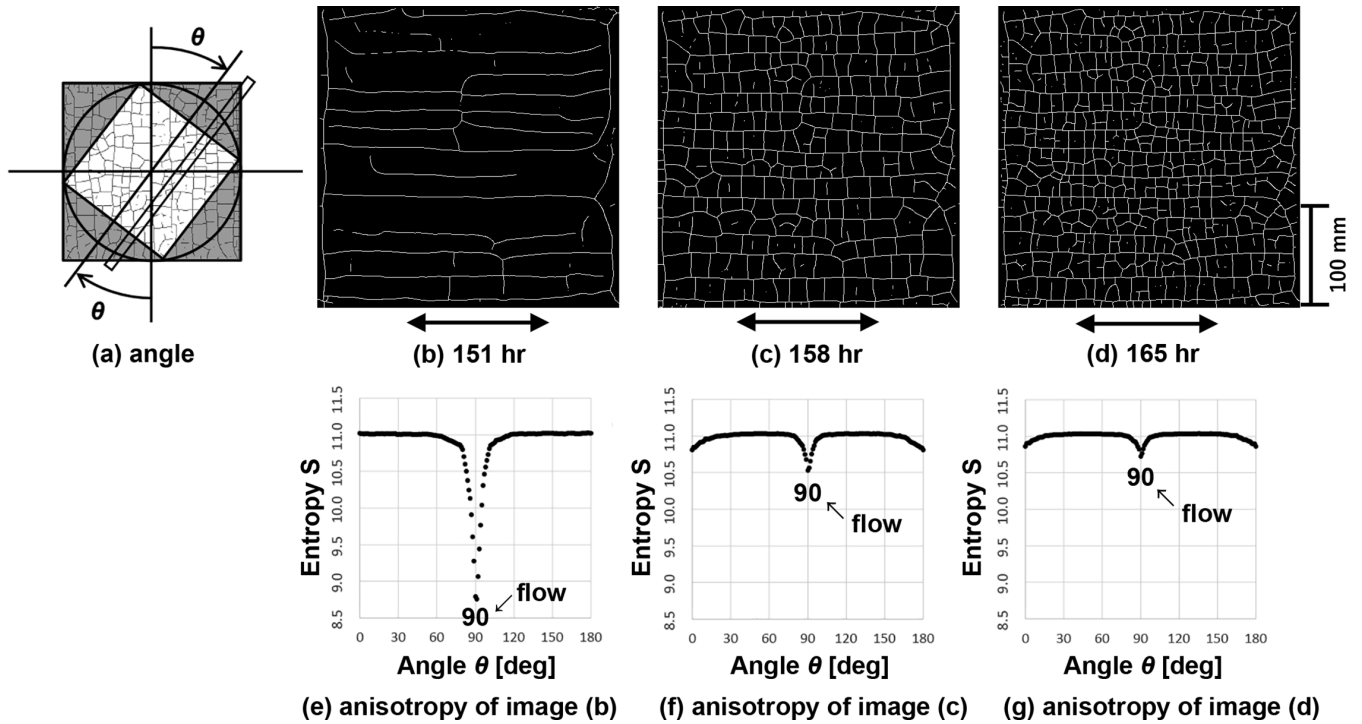


FIG. 6. Shannon’s information entropy S , which estimates the time evolution of striped desiccation crack pattern of paste of magnesium carbonate hydroxide shown in Figs. 1(b) and 5(c), the direction of which is parallel to its flow direction (memory effect of flow). (a) Angle θ of the direction along which we calculate S . Panels (b)–(d) show processed images of time evolution of striped desiccation crack pattern parallel to the flow direction. First a desiccation crack emerges at 144 hr after we stop vibrating the container and start drying the paste. The times of photo taking are 151 hr in panel (b), 158 hr in panel (c), and 165 hr in panel (d), respectively. Panel (d) corresponds to Fig. 5(c). First, primary cracks propagate straight and parallel to the flow direction in panel (b). As time passes, secondary cracks are created in the direction perpendicular to primary cracks. At the same time, randomness increases in the morphology of the crack pattern in panel (c). However, even though secondary cracks are produced and randomness increases, the anisotropy of primary striped cracks remains clearly until the end in panel (d). Panels (e)–(g) show S as functions of θ calculated from processed images (b)–(d). (e) S calculated from image (b) at 151 hr. The global minimum of S at $\theta = 90^\circ$ corresponds to “long and straight” primary cracks in the “right and left” direction ($\theta = 90^\circ$) induced by the memory of flow ($\theta = 90^\circ$). (f) S calculated from image (c) at 158 hr. The depth of the global minimum of S at $\theta = 90^\circ$ decreases. At the same time, the local minima of S at $\theta = 0^\circ$ and 180° emerge because secondary cracks are created in the direction perpendicular to primary cracks and randomness increases in the morphology of the crack pattern. (g) S calculated from image (d) at 165 hr, which corresponds to Fig. 5(f) expressed in a different vertical scale. Even though secondary cracks are produced and randomness in the morphology of the desiccation crack pattern increases, the global minimum of S at $\theta = 90^\circ$ does not vanish because the anisotropy of primary striped cracks still remains until the end.

Figure 6(a) shows the angle θ of the direction along which we calculate Shannon’s information entropy S . Then we estimate the preferential direction for cracks to propagate by the graph of S as a function of θ . Figures 6(b)–6(d) show processed images of the time evolution of the striped desiccation crack pattern parallel to the flow direction. The first crack emerges 144 hr after we stop vibrating the container and start to dry the paste at a room temperature of 25°C and a low humidity of 40%. The formation of new cracks lasts for about 20 hr. The times of photo-taking after we stop vibrating the container and start drying each paste are 151 hr in Fig. 6(b), 158 hr in Fig. 6(c), and 165 hr in Fig. 6(d). Figures 6(e)–6(g) show Shannon’s information entropies S as functions of an angle θ calculated from processed images of Figs. 6(b)–6(d). Figure 6(g) corresponds to Fig. 5(f), but in a different vertical scale.

First, primary cracks propagate straight and parallel to the flow direction as shown in Fig. 6(b). As time passes, secondary cracks are created in the direction perpendicular to

primary cracks. At the same time, randomness increases in the morphology of the crack pattern in Fig. 6(c), but even though secondary cracks are produced and randomness increases, the anisotropy of primary striped cracks remains clearly until the end in Fig. 6(d).

Next we reexamine the time evolution of the formation of striped crack patterns by calculating the time evolution of Shannon’s information entropy S . Figure 6(e) shows Shannon’s information entropy S as calculated from image Fig. 6(b) at 151 hr. The global minimum of S at $\theta = 90^\circ$ corresponds to “long and straight” primary cracks in the “right and left” direction ($\theta = 90^\circ$) induced by the memory of flow. Then Fig. 6(f) shows Shannon’s information entropy S calculated from image Fig. 6(c) at 158 hr. The depth of the global minimum of S at $\theta = 90^\circ$ decreases because randomness of the crack pattern morphology increases because of the formation of secondary cracks. At the same time, the local minima of S at $\theta = 0^\circ$ and 180° emerge because secondary cracks are created in the direction perpendicular to the primary cracks.

Finally, Fig. 6(g) shows Shannon's information entropy S calculated from image Fig. 6(d) at 165 hr. Even though secondary cracks are produced and randomness in the morphology of desiccation crack pattern increases, the global minimum of S at $\theta = 90^\circ$ does not vanish because the anisotropy of primary striped cracks remains until the end.

As explained above, the time evolution of the formation of striped crack patterns can be examined quantitatively by calculating the time evolution of Shannon's information entropies S as functions of an angle θ .

IV. EFFECTS OF ADDING STARCH TO THE CALCIUM CARBONATE PASTE

As described herein, we investigated the effects of adding starch to a plastic fluid that shows memory effects. CaCO_3 paste is a kind of paste which can remember its vibrational motion but which cannot remember its flow motion. First, we found that, after adding starch colloidal particles to CaCO_3 paste, CaCO_3 paste exhibits the ability to remember its flow motion. We also found that, even when we did not add starch colloidal particles to CaCO_3 paste, but added only a filtered solution of a starch colloidal suspension to CaCO_3 paste, the paste also exhibits the ability to remember its flow motion. We explain the experiment methods and present the experiment results in the following subsections.

A. Effects of adding starch colloidal particles to CaCO_3 paste

We use "Starch, potato" (Kanto Chemical Co. Inc., Tokyo, Japan) as starch colloidal particles to mix with CaCO_3 paste. The CaCO_3 colloidal particles are solid and difficult to dissolve in water. Therefore, they do not change their shapes and volumes in water. However, because starch colloidal particles absorb water inside, starch colloidal particles in water are soft and viscoelastic. They change their volume under pressure or shear. For that reason, we cannot estimate the density of starch colloidal particles in water precisely. The shape of each starch colloidal particle in water resembles that of a round particle, with $41\ \mu\text{m}$ median diameter of starch colloidal particles in water. These starch colloidal particles are charged negatively in water.

For the following experiments, we fix the volume of distilled water as 300 ml and change the amounts of CaCO_3 colloidal particles and starch colloidal particles which we add to 300 ml of distilled water to make a paste. Consequently, there are two main controlling parameters in the following systematic experiments. In Fig. 3 a solid volume fraction, i.e., a volume fraction of solid colloidal particles in a paste, is selected as a controlling parameter and is presented as a horizontal axis. Therefore, as a first controlling parameter for the following experiments we also choose a solid volume fraction of CaCO_3 colloidal particles in a CaCO_3 -water mixture, i.e., a volume of CaCO_3 colloidal particles divided by the sum of the volume of CaCO_3 colloidal particles and that of distilled water. A second controlling parameter we choose is the mass of dried starch colloidal particles which we add to the CaCO_3 -water mixture, which includes 300 ml of distilled water. Because starch colloidal particles absorb water and change their volume, we cannot use a volume of soft starch colloidal

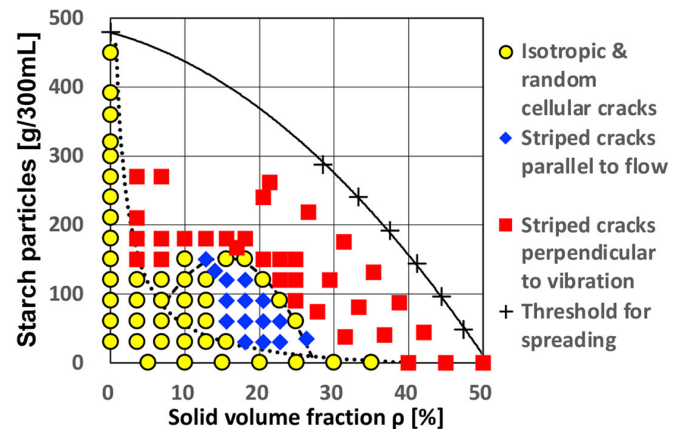


FIG. 7. Morphological phase diagrams of desiccation crack patterns of CaCO_3 pastes mixed with starch colloidal particles, expressed as a function of a solid volume fraction ρ of CaCO_3 colloidal particles in a CaCO_3 -water mixture and an amount of starch colloidal particles added to 300 ml of distilled water in the CaCO_3 -water mixture. A certain amount of CaCO_3 colloidal particles is mixed with 300 ml of distilled water so that the solid volume fraction of the CaCO_3 -water mixture becomes the value of ρ , then water-soluble starch is added to the CaCO_3 -water mixture. Each square acrylic container is 200 mm on each side. Each paste is vibrated horizontally at an amplitude of $r = 15\ \text{mm}$ and a frequency of $f = 60\ \text{rpm}$ for 5 min before drying. Open circles filled with yellow denote "isotropic and random cellular" desiccation crack patterns. Blue solid diamonds denote striped desiccation crack patterns, the direction of which is parallel to the direction of a flow induced by the vibration. Red solid squares denote striped desiccation crack patterns, the direction of which is perpendicular to the direction of a vibration. "Black plus symbols and a black solid curve" denote a threshold above which the paste cannot spread, even under a horizontal vibration, because of its strong plasticity. Therefore, the black solid curve corresponds to the yield stress line. A black broken curve represents a boundary between vibrational motion and flow motion of paste. A black dotted curve represents a boundary between "isotropic and random cellular" cracks and striped cracks induced by memory effects of paste. First, data on horizontal axis confirm that CaCO_3 paste can remember the direction of its vibrational motion but cannot remember its flow direction, as already presented in Fig. 3(b). Second, data on the vertical axis show that the starch colloidal suspension cannot remember any of its motions. Even though CaCO_3 paste and the starch colloidal suspension cannot remember their flow motions, the morphological phase diagram shows that, when CaCO_3 paste is mixed with starch colloidal particles, it can remember not only the direction of its vibrational motion but also its flow direction.

particles as a precise controlling parameter. Therefore, we decide to choose a mass of dried starch colloidal particle as a second controlling parameter.

Figure 7 shows the morphological phase diagram of the desiccation crack pattern of CaCO_3 paste mixed with starch colloidal particles. The horizontal axis shows the solid volume fraction of CaCO_3 colloidal particles in the CaCO_3 -water mixture. The vertical axis shows the mass of starch colloidal particles added to 300 ml of distilled water in the CaCO_3 -water mixture. As soon as a paste is poured into a square acrylic container with 200 mm on each side, the container is vibrated horizontally in one direction at a frequency of

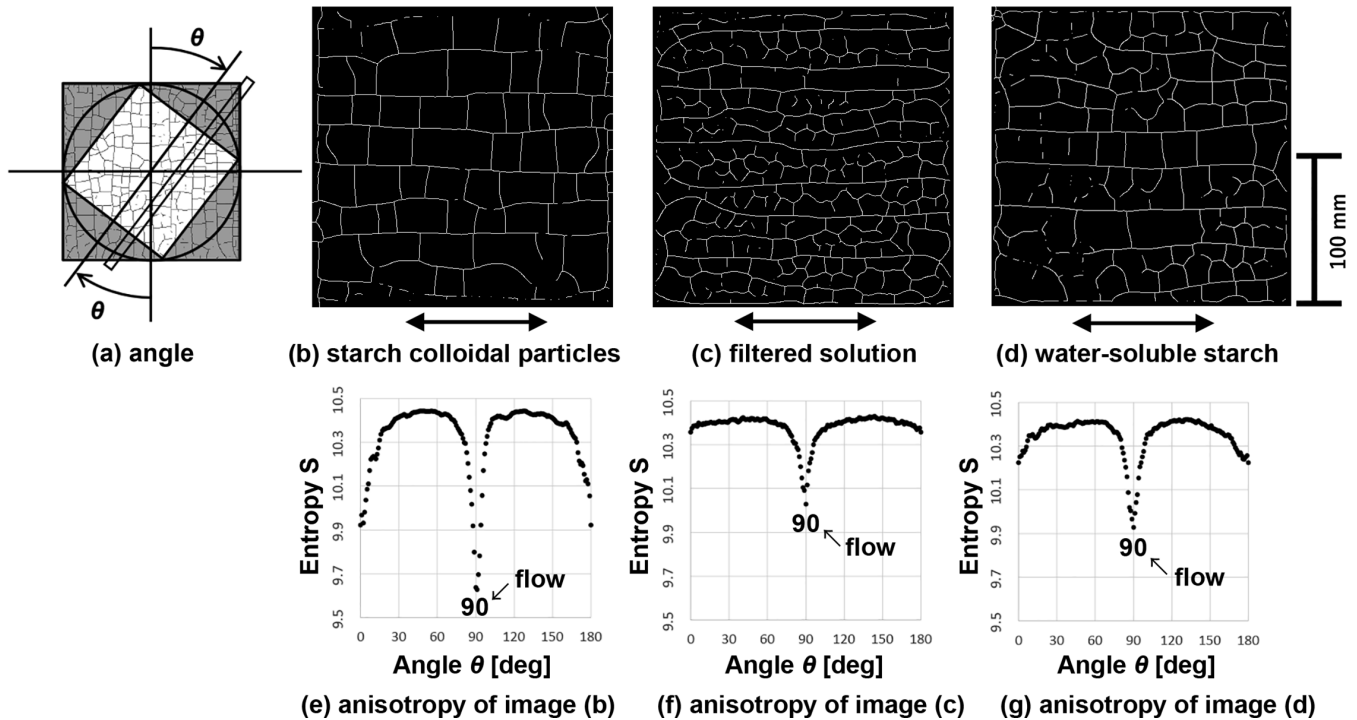


FIG. 8. Shannon's information entropy S , which estimates the effect of adding starch colloidal particles, a filtered solution of starch colloidal suspension, or water-soluble starch to CaCO_3 paste. (a) Angle θ of the direction along which we calculate S . Panels (b)–(d) show processed images of desiccation crack patterns of CaCO_3 pastes mixed with starch colloidal particles in (b), mixed with a filtered solution of starch colloidal suspension in (c), and mixed with a water-soluble starch in (d). In (b), 210 g of CaCO_3 colloidal particles is mixed with 300 ml of distilled water so that the solid volume fraction of the CaCO_3 -water mixture becomes $\rho = 20.5\%$. Then we add 90 g of starch colloidal particles into the CaCO_3 -water mixture to make a paste. In (c) 90 g of dried starch colloidal particles is mixed with 300 ml of distilled water to make a colloidal suspension of starch, and the starch colloidal particles are removed from the colloidal suspension of starch using filter paper and then using a disposable membrane filter unit. Consequently, we are able to extract 230 g of the filtered solution from the colloidal suspension of starch. Then 180 g of CaCO_3 colloidal particles is mixed with 230 g of the filtered solution to make a paste. The solid volume fraction of the paste is approximately 22.3%. In (d) 272 g of CaCO_3 colloidal particles is mixed with 300 ml of distilled water so that the solid volume fraction of the CaCO_3 -water mixture becomes $\rho = 25.0\%$, then we add 0.7 g of water-soluble starch into the CaCO_3 -water mixture to make a paste. Each paste is vibrated horizontally at an amplitude of $r = 15$ mm and a frequency of $f = 60$ rpm for 5 min before drying. Double-headed arrows indicate the direction along which each container is vibrated before drying. In all cases, i.e., in panels (b)–(d), striped desiccation crack patterns are obtained, with “long and straight” primary cracks propagating along the “right and left” direction, the direction of which is parallel to its flow direction, as shown in the morphological phase diagrams presented as Figs. 7 and 10(a). Therefore, it is apparent that CaCO_3 paste remembers its flow direction when mixed with starch colloidal particles, a filtered solution of starch colloidal suspension, or a water-soluble starch. Panels (e)–(g) show S as functions of θ which are calculated from processed image of (b) in (e), that of (c) in (f), and that of (d) in (g). In all cases, i.e., in panels (e)–(g), the global minimum of S at $\theta = 90^\circ$ corresponds to “long and straight” primary cracks in the “right and left” direction induced by the memory of flow. The local minima of S at $\theta = 0^\circ$ and 180° correspond to many short secondary cracks in the longitudinal direction.

$f = 60$ rpm and with an amplitude of $r = 15$ mm for 5 min. Therefore, the maximum strength of the absolute value of the acceleration induced by horizontal vibration is 0.59 m/s^2 . After halting the horizontal vibration of the container, the paste is kept still and dried at a room temperature (25°C) and at low humidity of 40%. The desiccation cracks emerge within a week.

As depicted in Fig. 7, when starch colloidal particles are not added to CaCO_3 paste as data on the horizontal axis, the CaCO_3 paste shows memory of vibration at the high solid volume fraction, whereas the paste shows only a “isotropic and random cellular” desiccation crack pattern with no memory of its motion at the low solid volume fraction. These results are the same as those presented in Fig. 3. Data shown on vertical axis indicate that the starch paste without CaCO_3 colloidal

particles exhibits no memory effect and that the desiccation cracks take only “isotropic and random cellular” structures, which are similar to a top view of columnar joints [8–13]. Furthermore, for the region where CaCO_3 colloidal particles and starch colloidal particles are mixed with distilled water to make a paste, the paste can remember the directions not only of vibration but also of flow, depending on the situations.

For example, Fig. 8 portrays the effects of adding starch colloidal particles to CaCO_3 paste in Figs. 8(b) and 8(e), a filtered solution of starch colloidal suspension to CaCO_3 paste in Figs. 8(c) and 8(f), and water-soluble starch to CaCO_3 paste in Figs. 8(d) and 8(g).

Figures 8(b) and 8(e) show 210 g of CaCO_3 colloidal particles mixed with 300 ml of distilled water to make a CaCO_3 -water mixture with a solid volume fraction of 20.5%,

then mixed with starch colloidal particles of 90 g, and vibrated horizontally before being dried. The CaCO_3 pastes mixed with starch colloidal particles remember their flow direction. A striped desiccation crack pattern is obtained, the direction of which is parallel to the flow direction induced by the horizontal vibration of the container. Figure 8(b) corresponds to a processed image of the striped desiccation crack pattern. Because the real inner size of the square container is 200 mm on each side, we rescale the inner size of the container in the image data as 2000 pixels \times 2000 pixels. Figure 8(e) corresponds to Shannon's information entropies S as a function of angle θ , which are calculated from a processed image of Fig. 8(b). In Fig. 8(e) the global minimum of S at $\theta = 90^\circ$ corresponds to "long and straight" primary cracks in the "right and left" directions induced by the memory of flow. The local minima of S at $\theta = 0^\circ$ and 180° correspond to many short secondary cracks in the longitudinal direction, which emerge to cut "long rectangles made by "long and straight" primary cracks" into small pieces.

To summarize, CaCO_3 paste can remember the direction of its vibrational motion but cannot remember the direction of its flow motion. However, by adding a proper amount of starch colloidal particles to the CaCO_3 paste, CaCO_3 paste attains the ability to remember its flow motion.

B. Effects of adding a filtered solution of a starch colloidal suspension to CaCO_3 paste

From our investigations conducted to date, we have realized that interparticle attractions among colloidal particles in water are dominant factors affecting a paste's ability to exhibit memory effects. For example, a water-poor CaCO_3 paste remembers the direction of its vibrational motion as a form of anisotropic dense network structure because of the short-ranged van der Waals interparticle attraction [39], but because CaCO_3 colloidal particles are positively charged in water, a water-medium CaCO_3 paste cannot remember its flow direction because long-ranged Coulombic repulsion prevents formation of an anisotropic dilute network structure that keeps the memory of flow. Therefore, CaCO_3 paste gains the ability to remember its flow direction when sodium chloride (NaCl) is added to it because the long-ranged Coulombic repulsion among positively charged CaCO_3 colloidal particles is screened by negatively charged Cl^- ions and the short-ranged van der Waals interparticle attraction among CaCO_3 colloidal particles becomes a dominant interaction among CaCO_3 colloidal particles [32].

As described in the preceding subsection, results indicated that, aside from adding sodium chloride, the addition of starch colloidal particles to CaCO_3 paste enables the paste to remember its flow direction. This finding suggests that the addition of starch colloidal particles also plays the same role as that of sodium chloride and leads to a situation in which attractive interactions become dominant among CaCO_3 colloidal particles. Consequently, the memory effect of flow is obtained. However, an important question arises.

When sodium chloride (NaCl) is added to CaCO_3 paste, it dissolves completely in water as a solvent. It is ionized as Na^+ ions and Cl^- ions. The Cl^- ions are distributed to screen Coulombic repulsion produced by positively charged

CaCO_3 colloidal particles [32]. However, because the median diameter of starch colloidal particles, 41 μm , is 10 times larger than the median diameter of CaCO_3 colloidal particles, which is 4.0 μm , it seems difficult for large starch colloidal particles to screen the Coulombic repulsion among small CaCO_3 colloidal particles. Therefore, we come to think that the memory of flow was not induced by starch colloidal particles. Something which dissolves from starch colloidal particles into the solution plays an important role of inducing attractive interaction among positively charged CaCO_3 colloidal particles and assists the formation of memory of flow.

To extract that material which dissolves from the starch colloidal particles into the solution, 90 g of dried starch colloidal particles was mixed with 300 ml of distilled water to make a colloidal suspension of starch; then the starch colloidal particles were removed from the colloidal suspension of starch using Grade 6 filter paper with 3.0 μm pore size (Whatman, GE Healthcare, Buckinghamshire, UK) and then using a disposable membrane filter unit DISMIC-13HP with 0.45 μm pore size (Advantec, Tokyo, Japan). Therefore, we can extract a filtered solution from the colloidal suspension of starch, i.e., a saccharide solution. Then 230 g of the filtered solution, i.e., a saccharide solution, is mixed with 180 g of CaCO_3 colloidal particles to produce a paste. The solid volume fraction of the paste is approximately 22.3% if one assumes that the filtered solution density can be regarded as 1.0 g/cm^3 . Immediately after the paste is poured into a square acrylic container of 200 mm on each side, the paste is vibrated horizontally in one direction at a frequency of $f = 60$ rpm and with an amplitude of $r = 15$ mm for 5 min; then the paste is kept still and dried until the desiccation crack formation ends.

The resultant desiccation crack pattern is portrayed in Fig. 8(c); Fig. 8(f) corresponds to Shannon's information entropies S as a function of an angle θ , which is calculated from the processed image of Fig. 8(c). As shown in Fig. 8(f), the global minimum of S at $\theta = 90^\circ$ corresponds to "long and straight" primary cracks in the "right and left" direction induced by the memory of flow. The local minima of S at $\theta = 0^\circ$ and 180° correspond to many short secondary cracks in the longitudinal direction. Consequently, Figs. 8(c) and 8(f) show that the addition of saccharide solution to CaCO_3 paste enables the paste to remember its flow direction.

Therefore, for the memory of flow, we need not add starch colloidal particles to CaCO_3 paste: merely adding a saccharide solution is sufficient for the purpose.

V. EFFECTS OF ADDING SACCHARIDE SOLUTIONS WITH DIFFERENT MOLECULAR WEIGHTS TO CALCIUM CARBONATE PASTE

This section presents description of our systematic experiments used to investigate the effects of adding saccharide solution to CaCO_3 paste by changing the molecular weights of saccharide in the saccharide solution.

A. Purpose of experiments conducted by adding saccharides to CaCO_3 paste

The experiments described in Sec. IV show that the addition of starch colloidal particles to CaCO_3 paste caused

TABLE I. Number average molecular weights (M_n), weight average molecular weights (M_w), and polydispersity indexes (M_w/M_n) of saccharides.

Saccharide	M_n	M_w	M_w/M_n
Starch, soluble, potato	21 000	149 000	7.1
Dextrin in dextrin hydrate	5700	34 000	6.0
Glucose	180	180	1.0

the emergence of memory of flow. They also showed that the cause of the memory of flow is not attributable to the addition of starch colloidal particles: saccharide solutions, i.e., saccharides which dissolved from the starch colloidal particles into water, play an important role in the formation of memory of flow.

For systematic investigation of the effects of adding saccharide solution to CaCO_3 paste on the memory formation of flow, we use saccharides with different molecular weights, such as water-soluble starch, dextrin, and glucose. To compare the anisotropy of desiccation crack patterns, we perform image analysis as presented in Sec. III. First, we analyze the desiccation crack pattern morphology exhibited by CaCO_3 paste mixed with water-soluble starch, i.e., a polysaccharide. Then, we analyze that of CaCO_3 paste mixed with dextrin, i.e., a polysaccharide with a lower molecular weight than that of water-soluble starch. Finally, we examine that of CaCO_3 paste mixed with glucose, a monosaccharide.

B. Experiment method of adding saccharides to CaCO_3 paste

The molecular weights of the polysaccharides used in the following experiments were measured using the method of gel filtration chromatography with High Performance Liquid Chromatography Prominence (Shimadzu Corp., Kyoto, Japan) [56]. As saccharides, we use water-soluble-starch called “Starch, soluble, potato” (Kanto Chemical Co. Inc., Tokyo, Japan), dextrin hydrate (Kanto Chemical Co. Inc., Tokyo, Japan), and glucose (Kanto Chemical Co. Inc., Tokyo, Japan). Table I shows number average molecular weights (M_n), weight average molecular weights (M_w), and polydispersity indexes (M_w/M_n) of saccharides which are used in our experiments. The results of the measurements described in Table I confirm that water-soluble starch contains the largest number average molecular weight of 21 000, and that dextrin contains the second largest number average molecular weight of 5700. Glucose has the smallest number average molecular weight of 180.

After preparing solutions of water-soluble starch, dextrin, and glucose dissolved in 300 ml of distilled water, we produced pastes by mixing the solution with CaCO_3 colloidal particles. Then we conducted systematic experiments by preparing pastes with “different solid volume fractions of CaCO_3 colloidal particles in CaCO_3 -water mixture” and “different saccharide concentrations in the solution.” Each paste is vibrated horizontally in one direction at a frequency of $f = 60$ rpm and with amplitude of $r = 15$ mm for 5 min, immediately after the paste is poured into the square acrylic container of 200 mm on each side. Therefore, the maximum strength of the absolute value of the acceleration induced by horizontal vibration is 0.59 m/s^2 . After vibration, the pastes

are kept still and are dried at room temperature (25°C) and under low humidity of 40%.

Next, the obtained crack images are analyzed using Shannon’s information entropy S presented in Sec. III. To derive the direction of anisotropy of the desiccation crack pattern induced by memory effect, we calculate the value of Shannon’s information entropy S as a function of a direction θ , which reveals the direction of “long and straight” primary cracks with the lowest value of Shannon’s information entropy S . If the direction of the anisotropic crack pattern is $\theta = 0^\circ$ and 180° , then the anisotropic crack pattern shows the emergence of memory of vibration. If the direction of the anisotropic crack pattern is $\theta = 90^\circ$, then the anisotropic crack pattern visualizes the emergence of memory of flow.

Here we show whether CaCO_3 pastes mixed with water-soluble starch, dextrin or glucose can remember the direction of their flow motions. In Fig. 9, 272 g of CaCO_3 colloidal particles is mixed with 300 ml of distilled water for each case, so that the solid volume fraction of the CaCO_3 -water mixture becomes $\rho = 25.0\%$. To the CaCO_3 -water mixture of $\rho = 25.0\%$, we add 0.7 g of water-soluble starch in Fig. 9(b), 0.8 g of dextrin in Fig. 9(c), and 0.5 g of glucose in Fig. 9(d), to produce the respective pastes. Here, water-soluble starch does not dissolve in water at room temperature. It dissolves in hot water, and, once it dissolves in hot water, it remains to be dissolved in water even when cooled to room temperature. Therefore, in our experiment, the mixture of water-soluble starch and distilled water is heated at 70°C beforehand; after water-soluble starch dissolves in hot water, the mixture is cooled to room temperature and is mixed with CaCO_3 colloidal particles.

For each case in Fig. 9, a paste flows when it is vibrated horizontally; then we dry these pastes. From Figs. 9(b) and 9(c), it is apparent that striped desiccation crack patterns are obtained and that “long and straight” primary cracks propagate along the “right and left” direction, which is parallel to its flow direction. Therefore, it is apparent that CaCO_3 paste remembers its flow direction when mixed with polysaccharides such as water-soluble starch and dextrin. By contrast, Fig. 9(d) shows that, even if it flows, CaCO_3 paste cannot remember its flow direction when mixed with glucose, i.e., a monosaccharide.

C. Morphological phase diagram of desiccation crack patterns of CaCO_3 paste mixed with saccharides

As described in this subsection, we present experimentally obtained results in a morphological phase diagram of desiccation crack patterns of CaCO_3 paste mixed with saccharides of different types, such as water-soluble starch, dextrin, or glucose. The crack pattern anisotropy is characterized by image analysis using Shannon’s information entropy S presented in Sec. III. Figure 10(a) depicts the morphological phase diagram of desiccation crack patterns of CaCO_3 paste mixed with water-soluble starch. Figure 10(b) shows a morphological phase diagram of desiccation crack patterns of CaCO_3 paste mixed with dextrin, a polysaccharide of lower molecular weight than that of water-soluble starch. Also, Fig. 10(c) shows the morphological phase diagram of desiccation crack patterns of CaCO_3 paste mixed with glucose, a monosaccharide. The horizontal axes in Figs. 10(a)–10(c) represent

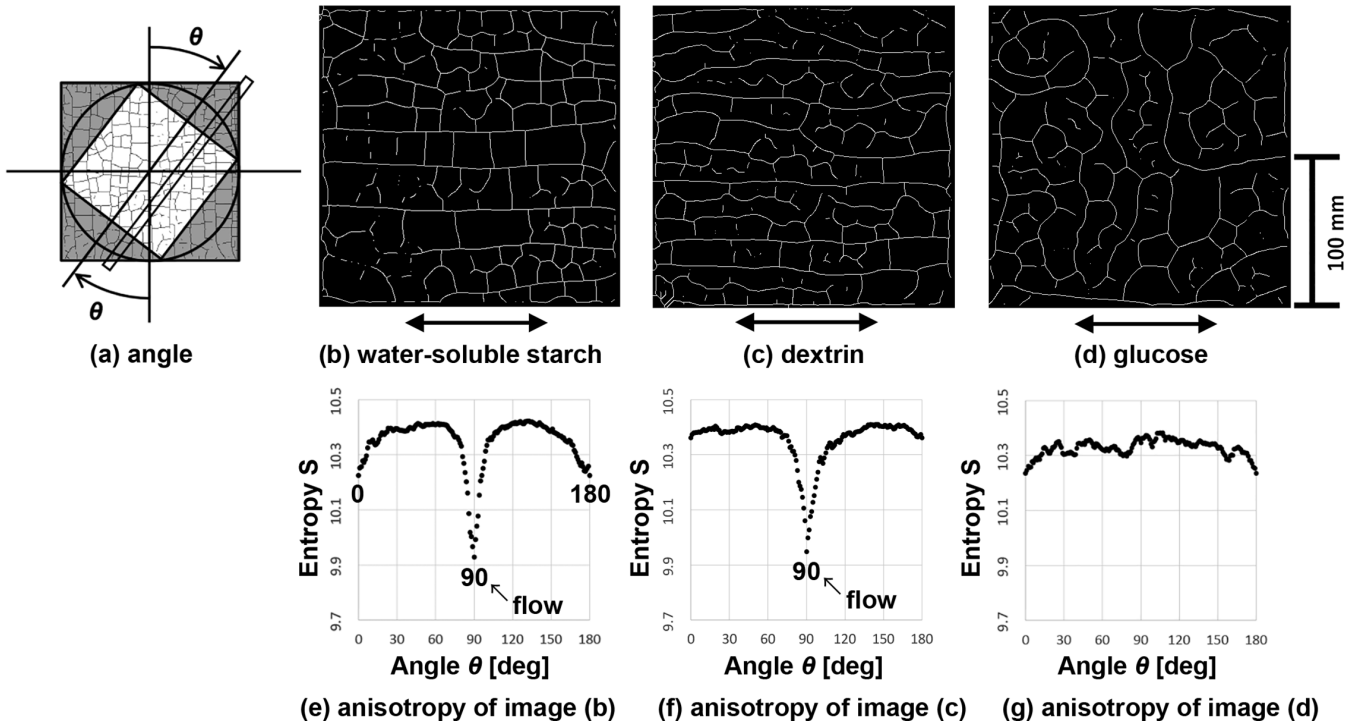


FIG. 9. Shannon’s information entropy S , which estimates the effect of adding water-soluble starch, dextrin, and glucose to CaCO_3 paste. (a) Angle θ of the direction along which we calculate S . Panels (b)–(d) show processed images of desiccation crack patterns of CaCO_3 pastes mixed with water-soluble starch in (b), mixed with dextrin in (c), and mixed with glucose in (d). Here 272 g of CaCO_3 colloidal particles is mixed with 300 ml of distilled water so that the solid volume fraction of the CaCO_3 -water mixture becomes $\rho = 25.0\%$. To the CaCO_3 -water mixture of $\rho = 25.0\%$, we add 0.7 g of water-soluble starch in (b), 0.8 g of dextrin in (c), and 0.5 g of glucose in (d), to produce the respective pastes. Each paste is vibrated horizontally at an amplitude of $r = 15$ mm and a frequency of $f = 60$ rpm for 5 min before drying. Double-headed arrows indicate the direction along which each container is vibrated before drying. In cases (b) and (c), striped desiccation crack patterns are obtained. “Long and straight” primary cracks propagate along the “right and left” direction, the direction of which is parallel to its flow along the “right and left” direction. Therefore, it is apparent that CaCO_3 paste remembers its flow direction when mixed with polysaccharides such as water-soluble starch and dextrin. By contrast, (d) shows that CaCO_3 paste cannot remember its flow direction when it is mixed with glucose, i.e., a monosaccharide. Panels (e)–(g) show S as functions of θ , as calculated from the processed image of (b) in (e), that of (c) in (f), and that of (d) in (g). For cases (e) and (f) in which “ CaCO_3 pastes mixed with water-soluble starch or dextrin” flow before drying, the global minimum of S at $\theta = 90^\circ$ corresponds to the “right and left” directions ($\theta = 90^\circ$) of “long and straight” primary cracks induced by the memory of flow ($\theta = 90^\circ$), and the local minima of S at $\theta = 0^\circ$ and 180° correspond to the longitudinal direction along which many short secondary cracks propagate to cut long rectangles made by “long and straight” primary cracks into small pieces. For a case (g) in which “ CaCO_3 paste mixed with a glucose” flows before drying, there is no global minimum of S , which means that there is no “long and straight” primary crack; the paste has no memory of its flow motion.

the solid volume fraction of CaCO_3 colloidal particles in the CaCO_3 -water mixture. The vertical axes show the amounts of saccharides added to 300 ml of distilled water in the CaCO_3 -water mixture.

In Figs. 10(a)–10(c), open circles filled with yellow denote “isotropic and random cellular” desiccation crack patterns. Also, blue solid diamonds denote striped desiccation crack patterns, the direction of which is parallel to the direction of a flow induced by the vibration. The red solid squares denote striped desiccation crack patterns, the direction of which is perpendicular to the direction of a vibration. “Black saltire cross symbols and a black solid curve” represent a threshold above which the paste cannot spread, even under a horizontal vibration, because of its strong plasticity. Therefore, the black solid curve corresponds to the yield stress line, on which the value of the maximum shear stress induced by a horizontal vibration equals that of the yield stress of the paste. A black broken curve represents a boundary between vibrational mo-

tion and flow motion of paste. A black dotted curve represents a boundary between striped cracks parallel to the flow and “isotropic and random cellular” cracks induced by turbulent flow motion.

Figure 10(a) shows the experimentally obtained result that, when a small amount of water-soluble starch, a longer polysaccharide with greater molecular weight, is added to CaCO_3 paste, a region of memory of flow appears at a solid volume fraction of 20%–30%; also a region of memory of vibration appears at a solid volume fraction of 30%–40% and the paste will not spread throughout the container at a solid volume fraction of greater than the plastic limit. Therefore, the CaCO_3 paste gains the ability to remember its flow direction when it is mixed with a small amount of water-soluble starch. It was also found that, when a large amount of water-soluble starch is added to CaCO_3 paste, the paste loses all of its ability to remember its motion. Only “isotropic and random-shaped” cracks appear in the drying process.

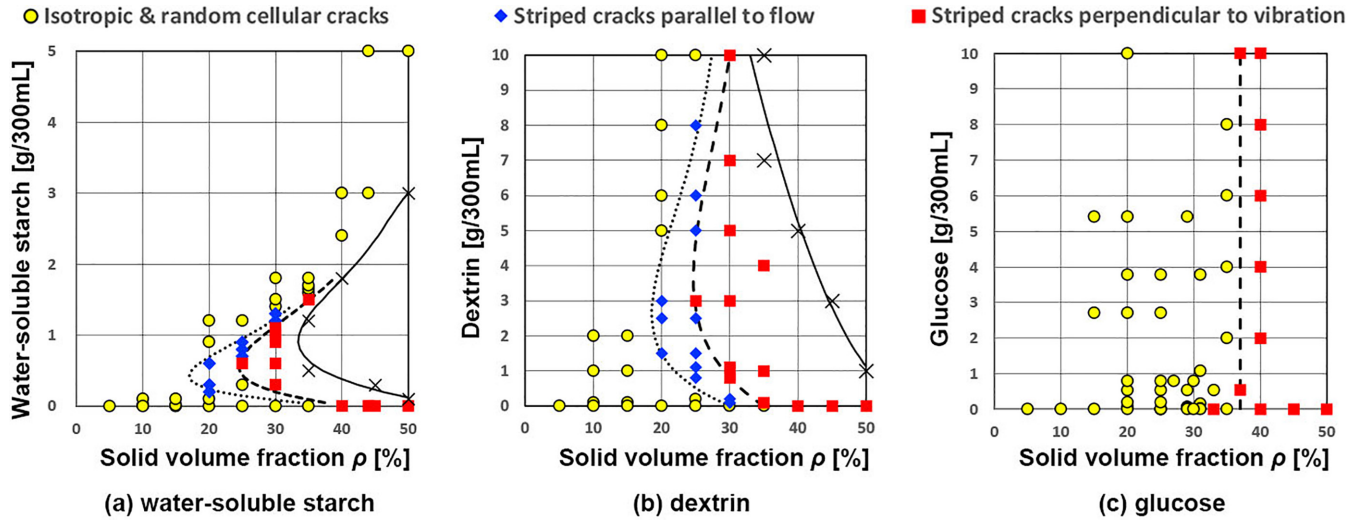


FIG. 10. Morphological phase diagrams of desiccation crack patterns of CaCO₃ pastes mixed with saccharides, expressed as functions of a solid volume fraction ρ of CaCO₃ colloidal particles in a CaCO₃-water mixture and an amount of saccharide added to 300 ml of distilled water in a CaCO₃-water mixture. A certain amount of CaCO₃ colloidal particles is mixed with 300 ml of distilled water so that the solid volume fraction of the CaCO₃-water mixture becomes the value of ρ . Then saccharide is added to the CaCO₃-water mixture. Each square acrylic container is 200 mm on each side. Each paste is vibrated horizontally at an amplitude of $r = 15$ mm and a frequency of $f = 60$ rpm for 5 min before drying. Open circles filled with yellow denote “isotropic and random cellular” desiccation crack patterns. Blue solid diamonds denote striped desiccation crack patterns, the direction of which is parallel to the direction of a flow induced by the vibration. Red solid squares denote striped desiccation crack patterns, the direction of which is perpendicular to the direction of a vibration. “Black saltire cross symbols and a black solid curve” denote a threshold above which the paste cannot spread, even under a horizontal vibration, because of its strong plasticity. Therefore, the black solid curve corresponds to the yield stress line. A black broken curve represents a boundary between vibrational motion and flow motion of paste; a black dotted curve represents a boundary between striped cracks parallel to flow and “isotropic and random cellular” cracks induced by turbulent flow motion. (a) CaCO₃ paste mixed with water-soluble starch (polysaccharide). (b) CaCO₃ paste mixed with dextrin (polysaccharide of lower molecular weight than water-soluble starch). (c) CaCO₃ paste mixed with glucose (monosaccharide). We find that when a proper amount of polysaccharide, such as water-soluble starch or dextrin, is added to CaCO₃ paste, the paste gains the ability to remember its flow direction, whereas the paste loses its ability to remember any of its motions when too much polysaccharides is added to CaCO₃ paste. We also find that the addition of longer polysaccharides, such as water-soluble starch, has a stronger influence on inducing the memory effect of flow and also on eliminating all memory effects. However, addition of glucose, i.e., monosaccharide, does not change memory effects because the monosaccharide length is insufficient to influence the memory effects of paste.

Figure 10(b) shows the experimentally obtained result that, when dextrin, a polysaccharide with a lower molecular weight than that of water-soluble starch, is added to CaCO₃ paste, a region of memory of flow appears at a solid volume fraction of 20%–30%; also a region of memory of vibration appears at a solid volume fraction of 30%–40% and the paste will not spread throughout the container at a solid volume fraction of greater than the plastic limit. Therefore, the CaCO₃ paste also gains the ability to remember its flow direction when it is mixed with a proper amount of dextrin. The amount of dextrin needed to gain the memory effect of flow is greater than that of water-soluble starch, a longer polysaccharide. The findings also confirmed that, when a small amount of water-soluble starch is added to CaCO₃ paste, the paste loses all of its ability to remember its motion; only “isotropic and random-shaped” cracks appear during the drying process, but the amount of dextrin needed to eliminate the memory effect is greater than that of water-soluble starch, a longer polysaccharide.

Figure 10(c) portrays the experimentally obtained result that the addition of glucose, a monosaccharide, to CaCO₃ paste did not cause any change in memory effects. We consider that the length of a monosaccharide is too short to change the interaction among CaCO₃ colloidal particles in water effectively.

D. Assisting and eliminating memory effects of paste by adding polysaccharides

Although CaCO₃ paste remembers the direction of its vibration, it cannot remember its flow direction. In this section, from morphological phase diagrams of desiccation crack patterns of CaCO₃ paste mixed with polysaccharide presented in Figs. 10(a)–10(c), we have found that, when CaCO₃ paste is mixed with a proper amount of polysaccharide, such as water-soluble starch or dextrin, the paste obtains the ability to remember its flow direction. By contrast, when CaCO₃ paste is mixed with any amount of monosaccharide, such as glucose, the paste cannot obtain the ability to remember its flow direction.

Results also indicate that the addition of small amount of polysaccharide assists CaCO₃ paste to remember its flow direction, whereas the addition of large amount of polysaccharide eliminates the memory effects of paste. As an example, in Fig. 11, we present results of experiments during which we increase the amount of water-soluble starch mixed with CaCO₃ paste.

We can confirm that the addition of polysaccharide can assist or eliminate memory effects of paste depending on the amount of polysaccharide added to the paste. When we compare the effects of adding equal amounts of polysaccharide to

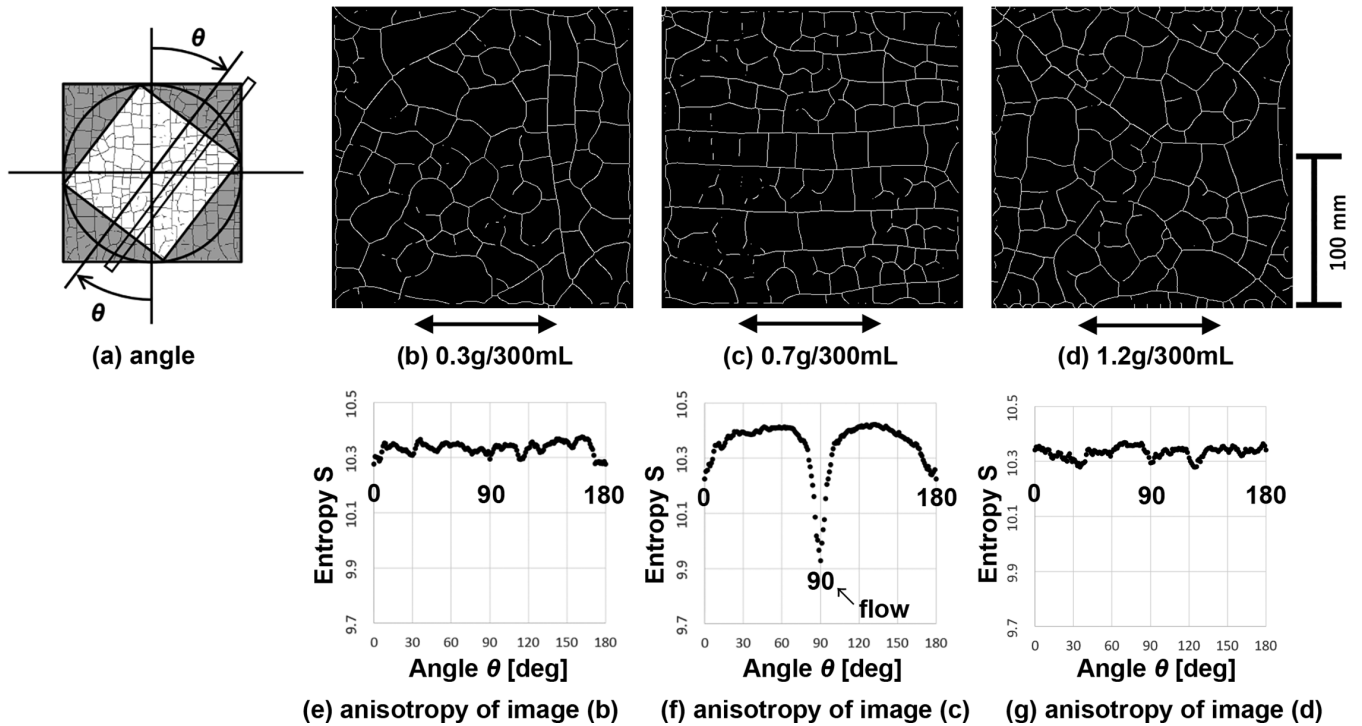


FIG. 11. Shannon’s information entropy S , which estimates the effect of adding different amounts of water-soluble starch to CaCO_3 paste. Here 272 g of CaCO_3 colloidal particles is mixed with 300 ml of distilled water so that the solid volume fraction of the CaCO_3 -water mixture becomes 25.0%. A certain amount of water-soluble starch is added to the CaCO_3 -water mixture. Each paste is vibrated horizontally along the double-headed arrow at an amplitude of $r = 15$ mm and a frequency of $f = 60$ rpm for 5 min before drying. (a) Angle θ of the direction along which we calculate S . Panels (b)–(d) show processed images of the desiccation crack pattern of CaCO_3 paste mixed with water-soluble starch. The amounts of water-soluble starch added to 300 ml of distilled water in a CaCO_3 -water mixture are 0.3 g/300 ml in (b), 0.7 g/300 ml in (c), and 1.2 g/300 ml in (d), respectively. The morphology of the desiccation crack pattern for each case is “isotropic and random cellular” in (b), striped cracks parallel to flow in (c), and “isotropic and random cellular” in (d), respectively. Also, (c) was already depicted in Figs. 8(d) and 9(b). Panels (e)–(g) show S as functions of θ calculated from processed images (b)–(d). (e) S calculated from image (b) of “isotropic and random cellular” cracks. For the case of an “isotropic and random cellular” crack pattern, there is no global minimum of S , which means that there is no “long and straight” primary crack and that the paste has no memory of its motions. (f) S calculated from image (c) of striped cracks along the “right and left” direction induced by memory of flow. The global minimum of S at $\theta = 90^\circ$ corresponds to “long and straight” primary cracks in the “right and left” direction induced by the memory of flow. The local minima of S at $\theta = 0^\circ$ and 180° correspond to many short secondary cracks in the longitudinal direction. (g) S calculated from image (d) of “isotropic and random cellular” cracks. As explained in (e) for the case of an “isotropic and random cellular” crack pattern, there is no “long and straight” primary crack; the paste has no memory of its motions. CaCO_3 paste of its solid volume fraction of $\rho = 25.0\%$ cannot remember any of its motion because of the lack of sufficient plasticity. Its desiccation crack pattern becomes “isotropic and random cellular.” When the small amount of water-soluble starch is added to CaCO_3 paste as in (b) and (e), it still cannot remember any of its motions. If the proper amount of water-soluble starch is added to CaCO_3 paste as in (c) and (f), then the paste gains the ability to remember its motion, such as a flow. However, if we add too much water-soluble starch to CaCO_3 paste as in (d) and (g), the paste loses its ability to remember any of its motions. Therefore, the memory effect of paste depends on how much polysaccharides is added to the paste.

CaCO_3 paste shown in Figs. 10(a) and 10(b), we realize that the addition of polysaccharide becomes more effective when the polysaccharide is longer and when it has greater molecular weight. The reasons for these mechanisms are discussed in the following sections.

VI. EFFECTS OF ADDING SACCHARIDES ON INTERPARTICLE INTERACTION AMONG COLLOIDAL PARTICLES

It was explained in Sec. V that CaCO_3 pastes mixed with polysaccharides, such as water-soluble starch or dextrin, obtain the ability to remember the flow direction. Our earlier reports have described that a necessary condition for a paste to

remember its flow direction is a situation in which a dominant interparticle interaction among colloidal particles in a solution is an attraction [32]. Therefore, in the following subsections, we describe experiments conducted to check whether the addition of polysaccharides to CaCO_3 pastes actually results in a situation where dominant interparticle interaction among CaCO_3 colloidal particles becomes an attraction. We also discover that the addition of glucose, i.e., a monosaccharide, does not result in a situation where dominant interparticle interaction among CaCO_3 colloidal particles becomes an attraction. For this reason, the addition of glucose does not influence the memory effects of paste. Finally, we compare all these results described in Secs. V and VI and elucidate the conditions for the emergence of memory effects of flow.

A. Method to investigate interparticle interaction by experimentation

To elucidate the dominant interparticle interactions among colloidal particles in saccharide solutions, we pour a dilute colloidal suspension into a test tube and observed the time evolution of the “floculation and sedimentation” process. The saccharide solution is prepared by dissolving a certain amount of saccharide in 50 ml of distilled water. Then we mix 10 g of CaCO_3 colloidal particles with the saccharide solution to make a dilute colloidal suspension. As saccharides to mix with CaCO_3 colloidal suspension, we use water-soluble starch, dextrin, and glucose. When the attractive force is the dominant interparticle interaction among colloidal particles in a solution, “floculation and sedimentation” occur rapidly. The test tube becomes transparent with a dense sedimentation layer of CaCO_3 colloidal particles at the bottom. However, when the repulsive force is the dominant interparticle interaction among colloidal particles in a solution, the sedimentation rate is slow; the test tube remains cloudy for a long while.

B. Effects of adding saccharides on interparticle interaction

Here we present experimentally obtained results from investigating the effects of adding saccharide on interparticle interaction among CaCO_3 colloidal particles in a solution. In the following experiments, the inner diameter of a test tube is 22 mm, the volume of water in each test tube is 50 ml, and the mass of CaCO_3 colloidal particles in each tube is 10 g. The photographs in Figs. 12–14 were taken 5 hr after pouring the colloidal suspension into the test tubes.

Figure 12 shows the effects of adding water-soluble starch, a longer polysaccharide with greater molecular weight, on interparticle interaction among CaCO_3 colloidal particles in a solution. In Fig. 12 the concentrations of water-soluble starch in the respective solutions are, from left to right, 0.0, 0.005, 0.01, 0.02, and 0.03 g/50 ml. When we do not mix water-soluble starch into the CaCO_3 solution, the test tube remains cloudy even at 5 hr after we pour the colloidal suspension into the test tube, because the dominant interparticle interaction is Coulombic repulsion caused by positively charged CaCO_3 colloidal particles [32]. When a proper amount of water-soluble starch is mixed with CaCO_3 solution, such as the situations of starch concentration of 0.005, 0.01, and 0.02 g/50 ml, we observe the sedimentation of CaCO_3 colloidal particles in the solution and the test tube becomes transparent. This result indicates that the attraction among CaCO_3 colloidal particles becomes dominant as we mix a proper amount of water-soluble starch with CaCO_3 solution. However, when too much water-soluble starch is mixed with CaCO_3 solution, such as the situation of starch concentration of 0.03 g/50 ml, sedimentation of the CaCO_3 colloidal particles in the solution is too slow, and thereby the test tube remains cloudy for a long while. This result indicates that the dominant interaction among CaCO_3 colloidal particles becomes repulsive when too much water-soluble starch is mixed with the CaCO_3 solution.

Figure 13 shows the effects of adding dextrin, a shorter polysaccharide with lower molecular weight, on interparticle interaction among CaCO_3 colloidal particles in a solution. The concentrations of dextrin in each solution in Fig. 13 are,

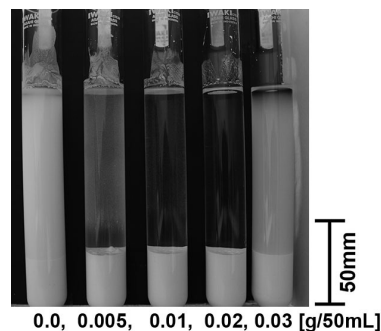


FIG. 12. Effects of adding water-soluble starch on interparticle interaction in a dilute suspension of CaCO_3 colloidal particles and water. The photograph is taken 5 hr after pouring the colloidal suspension into test tubes. Concentrations of water-soluble starch in each solution are, from left to right, 0.0, 0.005, 0.01, 0.02, and 0.03 g/50ml. The first test tube from the left shows that, when we do not mix water-soluble starch to CaCO_3 solution, the test tube remains cloudy even at 5 hr after pouring the colloidal suspension into the test tube, because the dominant interparticle interaction is Coulombic repulsion caused by positively charged CaCO_3 colloidal particles [32]. When a proper amount of water-soluble starch is mixed with the CaCO_3 solution, such as the situations of starch concentration 0.005, 0.01, and 0.02 g/50 ml, we observe the “floculation and sedimentation” of CaCO_3 colloidal particles in the solution and the test tube becomes transparent. This result indicates that the attraction among CaCO_3 colloidal particles becomes dominant as we mix a proper amount of water-soluble starch with the CaCO_3 solution. By contrast, when too much water-soluble starch is mixed with CaCO_3 solution, such as the situation of starch concentration 0.03 g/50 ml, we observe that the sedimentation of CaCO_3 colloidal particles in the solution is too slow and that the test tube remains cloudy. This result indicates that the dominant interaction among CaCO_3 colloidal particles becomes repulsive when we mix too much water-soluble starch with the CaCO_3 solution.

from left to right, 0.0, 0.005, 0.01, 0.02, 0.03, 0.10, 0.15, 0.20, 0.25, and 0.30 g/50 ml. The first test tube from the left in Fig. 13 shows that, when we do not mix dextrin to the CaCO_3 solution, the test tube remains cloudy, even at 5 hr after we pour the colloidal suspension into test tubes. When a proper amount of dextrin is mixed with CaCO_3 solution, such as the situations of dextrin concentration 0.10, 0.15, and 0.20 g/50 ml, we observe the “floculation and sedimentation” of CaCO_3 colloidal particles in the solution, and the test tube becomes transparent. This result indicates that the attraction among CaCO_3 colloidal particles becomes dominant as we mix a proper amount of dextrin with CaCO_3 solution. However, when too much dextrin is mixed with CaCO_3 solution, such as the situation of dextrin concentration 0.25 g/50 ml and more, the “floculation and sedimentation” of CaCO_3 colloidal particles in the solution are too slow, and thereby the test tube remains cloudy for a long while. This result indicates that the dominant interaction among CaCO_3 colloidal particles becomes repulsive when too much dextrin is mixed with the CaCO_3 solution.

From comparison of the experimentally obtained results obtained in Figs. 12 and 13, we understand that the addition of a proper amount of polysaccharide, such as water-soluble

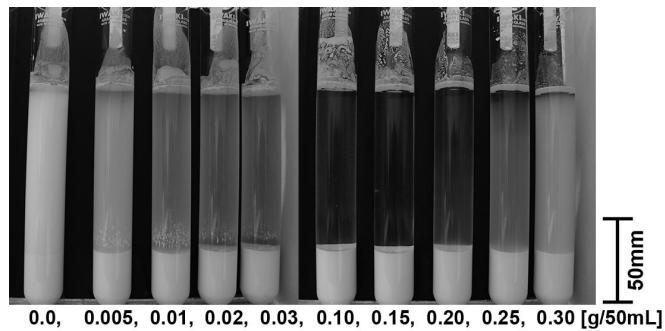


FIG. 13. Effects of adding dextrin on interparticle interaction in a dilute suspension of CaCO_3 colloidal particles and water. The photograph is taken 5 hr after pouring the colloidal suspension into test tubes. Concentrations of dextrin in each solution are, from left to right, 0.0, 0.005, 0.01, 0.02, 0.03, 0.10, 0.15, 0.20, 0.25, and 0.30 g/50ml. The first test tube from the left shows that, when we do not mix dextrin to the CaCO_3 solution, the test tube remains cloudy even at 5 hr after pouring the colloidal suspension into the test tube. When a proper amount of dextrin is mixed with CaCO_3 solution, such as the situations of dextrin concentration 0.10, 0.15, and 0.20 g/50ml, we observe the “floculation and sedimentation” of CaCO_3 colloidal particles in the solution and the test tube becomes transparent. This result indicates that the attraction among CaCO_3 colloidal particles becomes dominant as we mix a proper amount of dextrin with the CaCO_3 solution. By contrast, when too much dextrin is mixed with CaCO_3 solution, such as the situation of dextrin concentration 0.25 g/50ml and more, we observe that the sedimentation of CaCO_3 colloidal particles in the solution is too slow and that the test tube remains cloudy. This result indicates that the dominant interaction among CaCO_3 colloidal particles becomes repulsive when we mix too much dextrin with CaCO_3 solution. We also find that, to obtain the ability to remember its flow direction, CaCO_3 paste needs more mass concentration of dextrin than water-soluble starch. More additional mass concentration of dextrin is necessary to eliminate memory effects.

starch or dextrin, enables CaCO_3 paste to remember its flow direction. At the same time, the addition of too much polysaccharide eliminates the memory effects of paste. To obtain the ability to remember its flow direction, CaCO_3 paste needs more mass concentration of dextrin than water-soluble starch. Findings also indicate that a greater added mass concentration of dextrin is necessary to eliminate memory effects than that of water-soluble starch. These experimentally obtained results are explainable below by considering that dextrin is a shorter polysaccharide with lower molecular weight when compared with water-soluble starch, i.e., a longer polysaccharide with greater molecular weight.

Figure 14 shows the effects of adding glucose, a monosaccharide, on interparticle interaction in a dilute suspension of CaCO_3 colloidal particles and water. Even when the amount of glucose added to the CaCO_3 colloidal suspension is increased, all test tubes remain cloudy. This result indicates that the addition of monosaccharide is insufficient to influence the memory effects of paste. Therefore, Coulombic repulsion among positively charged CaCO_3 colloidal particles remains dominant even when glucose is added to the CaCO_3 colloidal suspension.

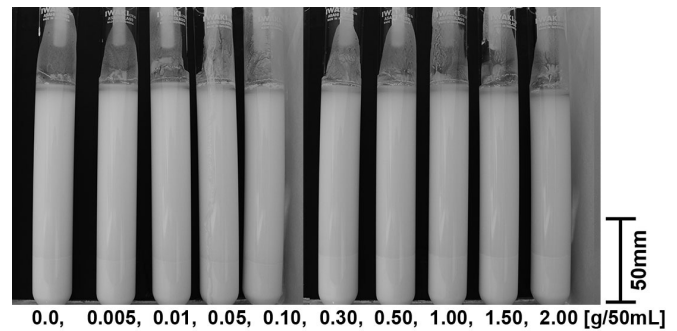


FIG. 14. Effects of adding glucose on interparticle interaction in a dilute suspension of CaCO_3 colloidal particles and water. The photograph is taken 5 hr after pouring the colloidal suspension into test tubes. Concentrations of glucose in each solution are, from left to right, 0.0, 0.005, 0.01, 0.05, 0.10, 0.30, 0.50, 1.00, 1.50, and 2.00 g/50ml. The first test tube from the left shows that, when we do not mix glucose to CaCO_3 colloidal suspension, the test tube remains cloudy, even at 5 hr after pouring the colloidal suspension into the test tube. When we check the “floculation and sedimentation” process in all test tubes, we understand that, even when the amount of glucose added to the CaCO_3 colloidal suspension is increased, all test tubes remain cloudy, indicating that Coulombic repulsion among CaCO_3 colloidal particles remains dominant even when glucose is added to the CaCO_3 colloidal suspension.

C. Comparison of interparticle interaction and memory effects

This subsection describes comparisons of experimentally obtained results obtained for interparticle interaction in Sec. VI with those of memory effects in Sec. V. The CaCO_3 paste is capable of remembering the direction of its vibrational motion, but it cannot remember its flow direction. The attraction should lead to a dominant interparticle interaction among CaCO_3 colloidal particles for the emergence of memory effect of flow [32].

Figures 9, 10(a), 10(b), and 11 in Sec. V show that, when CaCO_3 paste is mixed with polysaccharide such as water-soluble starch or dextrin, the paste becomes capable of remembering its flow direction. If more polysaccharide is added to the paste, then the paste loses the ability to remember the direction of its flow and also its vibrational motion. Figures 12 and 13 in Sec. VI show that, when a proper amount of polysaccharide is mixed with CaCO_3 solution, we observe the “floculation and sedimentation” of CaCO_3 colloidal particles in the solution; the test tube becomes transparent. This result indicates that the attraction among CaCO_3 colloidal particles becomes dominant as we mix a proper amount of polysaccharide with CaCO_3 solution. By contrast, when too much polysaccharide is mixed with CaCO_3 solution, we observe that the sedimentation of CaCO_3 colloidal particles in the solution becomes too slow. The test tube remains cloudy for a long while. This result indicates that the dominant interaction among CaCO_3 colloidal particles becomes repulsive when we mix too much polysaccharide with CaCO_3 solution.

These study findings also indicated that, to obtain the ability to remember its flow direction, CaCO_3 paste needs a greater mass concentration of dextrin than water-soluble starch. More additional mass concentration of dextrin is necessary to eliminate memory effects than that of water-soluble

starch. Table I shows that water-soluble starch is a longer polysaccharide with greater molecular weight, whereas dextrin is a shorter polysaccharide with lower molecular weight. Consequently, longer polysaccharides with greater molecular weight induce a memory effect of flow more readily than a shorter polysaccharide with lower molecular weight. The addition of an extra longer polysaccharide eliminates memory effects more readily than that of shorter saccharides.

By contrast, Fig. 10(c) in Sec. V shows that, even when glucose, a monosaccharide, is added to CaCO_3 paste, the paste still cannot remember its flow direction for any concentration of added glucose. Figure 14 in Sec. VI shows that all test tubes remain cloudy for all concentrations of glucose. Therefore, CaCO_3 colloidal particles disperse in the suspension for all concentrations of glucose because Coulombic repulsion is still a dominant interparticle interaction among charged colloidal particles. We infer that glucose, a monosaccharide, is too short and that its molecular weight is too low to induce an attractive interparticle interaction among CaCO_3 colloidal particles. For this reason, CaCO_3 paste cannot remember its flow direction, even when glucose is mixed with the paste.

Two important questions remain: why does the addition of polysaccharide, such as water-soluble starch and dextrin, induce the ability for a paste to remember its flow direction. Why does the addition of extra polysaccharide eliminate memory effects of flow and vibration? These mechanisms will be discussed in the next section.

VII. DISCUSSION

For this study, we added polysaccharide, such as water-soluble starch or dextrin, to CaCO_3 paste in Sec. V and found that the addition of polysaccharide enables the paste to remember the direction of its flow motion. “Flocculation and sedimentation” experiments described in Sec. VI showed that, by adding a small amount of polysaccharide to CaCO_3 paste, CaCO_3 colloidal particles in the test tube form sediment and that the test tube becomes transparent with a dense sedimentation layer of CaCO_3 colloidal particles at the bottom. These results indicate that the attractive interparticle interaction among CaCO_3 colloidal particles is induced by the addition of polysaccharide. Results also indicate that the flocculation of CaCO_3 colloidal particles attributable to the interparticle attraction results in the formation of clusters, which form sediment in a shorter time. These clusters formed by the interparticle attraction are inferred as the key to retaining the memory of their flow motion in the form of an anisotropic network structure.

Another question arises: why does the addition of polysaccharide induce the interparticle attraction among CaCO_3 colloidal particles in a solution and enable the paste to remember its flow direction? To understand the mechanism, we review the role of polymers added into a colloidal suspension [57–63].

When neutral polymers are mixed with a colloidal suspension, flocculation of colloidal suspension is induced mainly by two factors: by the depletion attractive force between colloidal particles and by the adsorption of the neutral polymer on both surfaces of two colloidal particles. The depletion attractive force between colloidal particles is induced due to the entropic

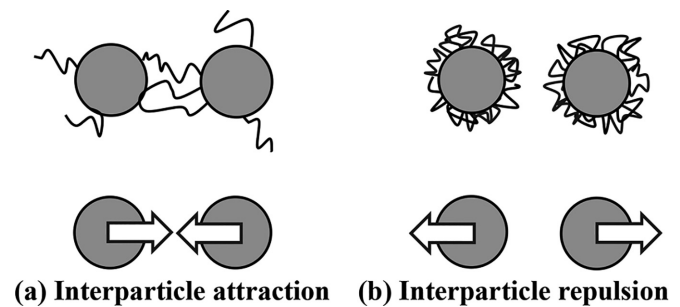


FIG. 15. Schematic illustrations of how the addition of soluble polysaccharides into a paste changes interparticle interactions between colloidal particles. (a) Interparticle attraction induced by a polymer bridge between colloidal particles at low polymer concentration. (b) Interparticle repulsion due to a wrapping of colloidal particles by polymers at high polymer concentration.

effect of polymers in dispersion, because the flocculation of colloidal particles gives the polymer larger effective volume for larger configurational entropy [57].

The adsorption of the neutral polymer on both surfaces of two colloidal particles is designated as polymer bridging: long linear polymers with high molecular weight can be adsorbed by more than one colloidal particle simultaneously, thereby forming a polymer bridge between colloidal particles. Schematic illustration of a polymer bridge between colloidal particles is shown in Fig. 15(a). The efficiency of flocculation of colloidal suspension by polymers is very sensitive to the molecular weight of polymers, the concentration of colloidal particles in colloidal suspension, and to the polymer concentration. The addition of small amount of long linear polymers with great molecular weight creates polymer bridges between colloidal particles, even at a low concentration of colloidal particles where interparticle distances between them are large. However, shorter linear polymers with lower molecular weight are less effective at polymer bridging because bridging via shorter linear polymers requires colloidal particles to approach each other more closely. Therefore, as the concentration of colloidal particles increases, polymer bridging becomes more effective because the interparticle distance between colloidal particles becomes smaller [59,60,62].

It is noteworthy that flocculation of colloidal suspension by polymer bridging is conducted only at low polymer concentrations. At low polymer concentrations, colloidal particles are only partially covered with adsorbed polymer. Therefore there are many opportunities for polymer bridging between different colloidal particles; flocculation of colloidal suspension occurs. As the polymer concentration increases, however, most of the surface of each colloidal particle becomes covered with its surrounding polymers, as is shown in Fig. 15(b). Consequently, the chances of polymer bridging between different colloidal particles vanish and flocculation of colloidal suspension does not occur [61,62].

Now we examine our experimentally obtained results presented in Secs. IV, V, and VI and assess how the addition of polysaccharides to CaCO_3 colloidal suspension influences the memory effects of paste. As reviewed above, for the role of polymers added to colloidal suspension, we infer that the addition of a small amount of polysaccharide causes polymer

bridging: polysaccharides in the solution are adsorbed onto the surfaces of CaCO_3 colloidal particles via attractive interactions, such as hydrogen bonding, and form polymer bridges between them, as is schematically shown in Fig. 15(a). As a first example, morphological phase diagrams of desiccation crack patterns of CaCO_3 pastes mixed with polysaccharides, as shown in Fig. 10 of Sec. V, portray that CaCO_3 paste mixed with polysaccharide, such as water-soluble starch or dextrin, has the ability to remember its flow direction. By contrast, CaCO_3 paste mixed with monosaccharide, i.e., glucose, has no ability to remember its flow direction. As a second example, when we compare situations in which we add polysaccharides of different types to CaCO_3 paste, such as water-soluble starch and dextrin, it is apparent that adding water-soluble starch is more effective than adding dextrin in assisting memory effects of flow. These experimentally obtained results are consistent with the fact that the polymer bridging efficiency is enhanced when the molecular weight of polymers is greater. Therefore, the addition of higher concentration of smaller polymers is not equivalent to the addition of low concentration of large polymers, because the addition of smaller polymers, such as glucose, cannot induce memory effect of flow even if we add higher amount of glucose. The polymer should be long enough to form polymer bridges between colloidal particles.

We can also reexamine the role of polysaccharides added to a CaCO_3 colloidal suspension from experimentally obtained results presented in Sec. VI. Comparison of Figs. 12–14, shows that the addition of a small amount of polysaccharide can induce attractive force between CaCO_3 colloidal particles, which becomes dominant among interparticle interactions and which results in a transparent test tube with a dense sedimentation layer at the bottom, although the addition of monosaccharide cannot induce attractive force between CaCO_3 colloidal particles. The experimentally obtained results presented in Sec. VI also suggest that the addition of water-soluble starch is more effective than that of dextrin for assisting the “floculation and sedimentation” processes. Therefore, we infer that polymer bridging via polysaccharides can play a role in the interparticle attraction necessary for the formation of clusters which can keep the memory of flow.

Next, we examine the results obtained when the amount of polysaccharide added to CaCO_3 paste is increased further. From viewing the morphological phase diagrams of desiccation crack patterns of CaCO_3 pastes mixed with polysaccharide, such as water-soluble starch or dextrin, shown in Figs. 10(a) and 10(b), one realizes that, as we increase the polymer concentration from 0 g/300 ml, the paste gains the ability to remember its flow motion. However, if the polymer concentration exceeds a threshold value, then the paste loses its ability to remember its motions not only of flow but also of vibration. As shown in Figs. 12 and 13, when a small amount of polysaccharide is added, the attraction between CaCO_3 colloidal particles becomes dominant and thereby the test tube becomes transparent. However, when the polysaccharide amount is increased further, the repulsion between CaCO_3 colloidal particles again becomes dominant and thereby the test tube remains cloudy for a long while.

These experimentally obtained results are consistent with the explanation of adsorption of polysaccharides on the

surface of colloidal particles. The interparticle interaction between CaCO_3 colloidal particles can be attractive or repulsive depending on the amount of added polysaccharide: attraction between colloidal particles becomes dominant when the amount of added polysaccharide is small; repulsion between colloidal particles becomes dominant when the amount of added polysaccharide is large. The idea of adsorption of polysaccharides on the surface of colloidal particles can explain that a small amount of adsorption of polymer on the surface of colloidal particles might permit the polymer bridging of colloidal particles leading to flocculation. However, higher amounts of adsorption engender stabilization, i.e., the addition of a large amount of polysaccharide causes polysaccharides in the solution to adsorb and to cover the surface of colloidal particles, thereby causing steric repulsion between colloidal particles [62], as is schematically shown in Fig. 15(b). Results suggest that, because of the steric repulsion between CaCO_3 colloidal particles, the memory effects of flow and vibration are eliminated when too much polysaccharide is added to CaCO_3 paste.

We note that the entropic effect of polymers in dispersion induces the depletion attractive force among colloidal particles. Thus, we consider that this depletion attractive force also assists the formation of memory effect of flow in paste [64]. However, the entropic effect of polymers in dispersion cannot induce repulsive interaction between colloidal particles even when we increase the amount of polysaccharide which we add to CaCO_3 paste. Therefore, the adsorption of polysaccharides on the surface of colloidal particles plays a dominant role in a transition from assisting to eliminating memory effects of paste.

We consider that results presented in this manuscript are not limited to the situation when soluble polysaccharide is added to a paste. We conjecture that the results are more general, i.e., the addition of proper amounts of long adsorbing polymers assists and eliminates memory effects of paste, and this conjecture should be verified in future problem.

VIII. CONCLUSIONS

By experimentation, we investigated how the memory effects of paste are influenced by adding saccharides to a paste. Results show that the addition of polysaccharides can assist and eliminate the memory effects of paste by controlling the amounts of polysaccharides added to the paste.

First, to characterize the anisotropy of desiccation crack patterns induced by the memory effects of paste, we proposed a method of image analysis to quantify the strength and the direction of the anisotropy of crack patterns using Shannon’s information entropy.

Then we reported results of our experiments, for which we added starch colloidal particles to CaCO_3 paste. From our series of studies conducted to date, we had confirmed that CaCO_3 paste can remember the direction of its vibrational motion, but it cannot remember the direction of its flow motion. Results indicate that the addition of starch colloidal particles to CaCO_3 paste induces the paste to remember its flow motion.

Next, we performed experiments to add water-soluble polysaccharide, such as water-soluble starch or dextrin, to

CaCO₃ paste, which revealed that the addition of small amounts of polysaccharide to CaCO₃ paste assists the paste to remember its flow motion. However, the addition of glucose, i.e., monosaccharide, cannot assist the paste to remember its flow motion. Starch colloidal particles are apparently not necessary to assist memory effects of flow. Some ingredients which dissolve from starch colloidal particles into a solution, i.e., sufficiently long water-soluble polysaccharides with sufficiently great molecular weight, play an important role in assisting the flow memory effect. Moreover, findings indicate that the addition of a large amount of polysaccharide prevents formation of flow memory and vibrational motion memory, while eliminating memory effects of paste.

We then performed “floculation and sedimentation” experiments to elucidate the interparticle interaction among CaCO₃ colloidal particles in a solution, which revealed that, in an aqueous solution with low polysaccharide concentration, CaCO₃ colloidal particles flocculate each other and form a sediment quickly. In an aqueous solution with a high polysaccharide concentration, a longer time is necessary for “floculation and sedimentation.”

The addition of small amounts of polysaccharides to CaCO₃ paste is inferred as inducing polymer bridging between colloidal particles as interparticle attraction. It helps to produce a macroscopic network structure that keeps the memory of its flow motion, and thereby assists the formation of memory of flow. By contrast, the addition of large

amounts of polysaccharides induces interparticle repulsion, which prevents the formation of all types of memory effects because the addition of a large amount of polysaccharide causes polysaccharides in the solution to adsorb and to cover the colloidal particle surface, causing steric repulsion among colloidal particles.

To summarize, results obtained from this study demonstrate that the addition of polysaccharides to a paste can change interparticle interactions among colloidal particles in the paste. It can assist and eliminate the memory effects of paste depending on the amount of polysaccharides added to the paste. Therefore, our method of adding polysaccharides to a paste is applicable to controlling mechanical properties of pastes by tuning the memory effects of paste under the addition of proper amounts of water-soluble polysaccharides.

ACKNOWLEDGMENTS

We acknowledge S. Kitsunezaki, Ooshida Takeshi, M. Otsuki, T. Mizuguchi, T. Yamazaki, W. Odagiri, S. Ito, F. Kun, and L. Goehring for valuable discussions. We would also like to acknowledge T. Okuzono and J. Yamanaka for helping us to measure Zeta potential of colloidal particles in a solution. This research was supported by JSPS Grant-in-Aid for Scientific Research [KAKENHI Grant No. JP20K03886], HAS-JSPS Joint Research Project, and International Exchange Scheme between the Royal Society and JSPS.

-
- [1] H. J. Herrmann and S. Roux (eds.), *Statistical Models for the Fracture of Disordered Media* (North-Holland, Amsterdam, 1990).
- [2] T. Ishii and M. Matsushita, *J. Phys. Soc. Jpn.* **61**, 3474 (1992).
- [3] L. Oddershede, P. Dimon, and J. Bohr, *Phys. Rev. Lett.* **71**, 3107 (1993).
- [4] A. Yuse and M. Sano, *Nature (London)* **362**, 329 (1993).
- [5] M. Marder, *Phys. Rev. E* **49**, R51 (1994).
- [6] Y. Hayakawa, *Phys. Rev. E* **49**, R1804 (1994).
- [7] S.-I. Sasa, K. Sekimoto, and H. Nakanishi, *Phys. Rev. E* **50**, R1733 (1994).
- [8] G. Müller, *J. Volcanol. Geotherm. Res.* **86**, 93 (1998).
- [9] A. Toramaru and T. Matsumoto, *J. Geophys. Res.* **109**, B02205 (2004).
- [10] L. Goehring and S. Morris, *Europhys. Lett.* **69**, 739 (2005).
- [11] T. Mizuguchi, A. Nishimoto, S. Kitsunezaki, Y. Yamazaki, and I. Aoki, *Phys. Rev. E* **71**, 056122 (2005).
- [12] L. Goehring, *Phil. Trans. R. Soc. A* **371**, 20120353 (2013).
- [13] L. Goehring, A. Nakahara, T. Dutta, S. Kitsunezaki, and S. Tarafdar, *Desiccation Cracks and their Patterns: Formation and Modelling in Science and Nature* (Wiley-VCH, Weinheim, Germany, 2015).
- [14] A. Groisman and E. Kaplan, *Europhys. Lett.* **25**, 415 (1994).
- [15] Y. Brechet, D. Bellet, and Z. Neda, *Solid State Phenomena* **42–43**, 247 (1995).
- [16] C. Allain and L. Limat, *Phys. Rev. Lett.* **74**, 2981 (1995).
- [17] S. Kitsunezaki, *Phys. Rev. E* **60**, 6449 (1999).
- [18] R. Blanc and H. van Damme, in *Mobile Particulate Systems*, NATO Advanced Study Institute Ser. E, Vol. 287, edited by E. Guazzelli and L. Oger (Kluwer, Dordrecht, 1995), p. 129.
- [19] H. A. Barnes, *J. Rheol.* **33**, 329 (1989).
- [20] A. J. Liu and S. R. Nagel, *Nature (London)* **396**, 21 (1998).
- [21] R. L. Hoffman, *J. Rheol.* **42**, 111 (1998).
- [22] C. B. Holmes, M. E. Cates, M. Fuchs, and P. Sollich, *J. Rheol.* **49**, 237 (2005).
- [23] T. F. Tadros, *Rheology of Dispersions* (Wiley-VCH, Weinheim, Germany, 2010).
- [24] J. Mewis and N. J. Wagner, *Colloid Suspension Rheology* (Cambridge University Press, Cambridge, 2012).
- [25] A. Nakahara and Y. Matsuo, *J. Phys. Soc. Jpn.* **74**, 1362 (2005).
- [26] A. Nakahara and Y. Matsuo, *J. Stat. Mech.* (2006) P07016.
- [27] A. Nakahara and Y. Matsuo, *Phys. Rev. E* **74**, 045102(R) (2006).
- [28] M. Otsuki, *Phys. Rev. E* **72**, 046115 (2005).
- [29] O. Takeshi, *Phys. Rev. E* **77**, 061501 (2008).
- [30] O. Takeshi, *J. Phys. Soc. Jpn.* **78**, 104801 (2009).
- [31] A. Nakahara, Y. Shinohara, and Y. Matsuo, *J. Phys.: Conf. Ser.* **319**, 012014 (2011).
- [32] Y. Matsuo and A. Nakahara, *J. Phys. Soc. Jpn.* **81**, 024801 (2012).
- [33] H. Nakayama, Y. Matsuo, Ooshida Takeshi, and A. Nakahara, *Eur. Phys. J. E* **36**, 1 (2013).
- [34] S. Kitsunezaki, A. Nakahara, and Y. Matsuo, *Europhys. Lett.* **114**, 64002 (2016).
- [35] Z. Halasz, A. Nakahara, S. Kitsunezaki, and F. Kun, *Phys. Rev. E* **96**, 033006 (2017).

- [36] S. Kitsunozaki, A. Sasaki, A. Nishimoto, T. Mizuguchi, Y. Matsuo, and A. Nakahara, *Eur. Phys. J. E* **40**, 88 (2017).
- [37] A. Nakahara, T. Hiraoka, R. Hayashi, Y. Matsuo, and S. Kitsunozaki, *Phil. Trans. R. Soc. A* **377**, 20170395 (2019).
- [38] R. Sztatmari, Z. Halasz, A. Nakahara, S. Kitsunozaki, and F. Kun, *Soft Matter* **17**, 10005 (2021).
- [39] S. Kitsunozaki, A. Nishimoto, T. Mizuguchi, Y. Matsuo, and A. Nakahara, *Phys. Rev. E* **105**, 044902 (2022).
- [40] J. Morita and M. Otsuki, *Eur. Phys. J. E* **44**, 106 (2021).
- [41] D. Mal, S. Sinha, T. R. Middy, and S. Tarafdar, *Physica A* **384**, 182 (2007).
- [42] L. Pauchard, F. Elias, P. Boltenhagen, A. Cebers, and J. C. Bacri, *Phys. Rev. E* **77**, 021402 (2008).
- [43] A. T. Ngo, J. Ricardi, and M. P. Pileni, *Nano Lett.* **8**, 2485 (2008).
- [44] A. T. Ngo, J. Ricardi, and M. P. Pileni, *J. Phys. Chem. B* **112**, 14409 (2008).
- [45] T. Khatun, M. D. Choudhury, T. Dutta, and S. Tarafdar, *Phys. Rev. E* **86**, 016114 (2012).
- [46] T. Khatun, T. Dutta, and S. Tarafdar, *Applied Clay Science* **86**, 125 (2013).
- [47] T. Khatun, T. Dutta, and S. Tarafdar, *Langmuir* **29**, 15535 (2013).
- [48] H. Lama, V. R. Dugyala, M. G. Basavaraj, and D. K. Satapathy, *Phys. Rev. E* **94**, 012618 (2016).
- [49] A. Fall, F. Bertrand, G. Ovaries, and D. Bonn, *J. Rheol.* **56**, 575 (2012).
- [50] E. Brown and H. M. Jaeger, *J. Rheol.* **56**, 875 (2012).
- [51] P. Nandakishore and L. Goehring, *Soft Matter* **12**, 2253 (2016).
- [52] Y. Akiba and H. Shima, *J. Phys. Soc. Jpn.* **88**, 024001 (2019).
- [53] C. E. Shannon, *Bell Syst. Tech. J.* **27**, 379 (1948).
- [54] C. E. Shannon, *Bell Syst. Tech. J.* **27**, 623 (1948).
- [55] T. Y. Zhang and C. Y. Suen, *Comm. ACM* **27**, 236 (1984).
- [56] Measurement of number average molecular weight of saccharides was performed by UBE Scientific Analysis Laboratory (Tokyo, Japan) under the method of gel filtration chromatography using High Performance Liquid Chromatography Prominence (Shimadzu, Kyoto, Japan).
- [57] S. Asakura and F. Oosawa, *J. Chem. Phys.* **22**, 1255 (1954).
- [58] W. B. Russel, D. A. Saville, and W. R. Schowalter, *Colloidal Dispersions* (Cambridge University Press, Cambridge, 1989).
- [59] J. Gregory, *Colloids Surf.* **31**, 231 (1988).
- [60] V. Chaplain, M. L. Janex, F. Lafuma, C. Graillat, and R. Audebert, *Colloid Polym. Sci.* **273**, 984 (1995).
- [61] N. G. Hoogeveen, M. A. C. Stuart, and G. J. Fleer, *Colloids Surf., A* **117**, 77 (1996).
- [62] I. D. Morrison and S. Ross, *Colloidal Dispersions: Suspensions, Emulsions, and Foams* (Wiley-VCH, Weinheim, Germany, 2002).
- [63] H.-J. Butt, K. Graf, and M. Kappl, *Physics and Chemistry of Interfaces*, 3rd revised and enlarged edition (Wiley-VCH, Weinheim, Germany, 2013).
- [64] N. Cawdery, A. Milling, and B. Vincent, *Colloids Surf., A* **86**, 239 (1994).